

THE INCIPIENT LAYER OF WAX DEPOSIT

Tunya Ketjuntiwa

A Thesis Submitted in Partial Fulfillment of the Requirements
for the Degree of Master of Science
The Petroleum and Petrochemical College, Chulalongkorn University
in Academic Partnership with
The University of Michigan, The University of Oklahoma,
Case Western Reserve University, and Institut Français du Pétrole
2017

บทคัดย่อและแฟ้มข้อมูลฉบับเต็มของวิทยานิพนธ์ตั้งแต่ปีการศึกษา 2554 ที่ให้บริการในคลังปัญญาจุฬาฯ (CUIR)
เป็นแฟ้มข้อมูลของนิสิตเจ้าของวิทยานิพนธ์ที่ส่งผ่านทางบัณฑิตวิทยาลัย

The abstract and full text of theses from the academic year 2011 in Chulalongkorn University Intellectual Repository (CUIR)
are the thesis authors' files submitted through the Graduate School.

Thesis Title: The Incipient Layer of Wax Deposit
By: Ms. Tunya Ketjuntiwa
Program: Petroleum Technology
Thesis Advisors: Asst. Prof. Pomthong Malakul
Prof. H. Scott Fogler

Accepted by The Petroleum and Petrochemical College, Chulalongkorn University, in partial fulfillment of the requirements for the Degree of Master of Science.

..... College Dean
(Prof. Suwabun Chirachanchai)

Thesis Committee:

.....
(Asst. Prof. Pomthong Malakul)

.....
(Prof. H. Scott Fogler)

.....
(Prof. Sumaeth Chavadej)

.....
(Asst. Prof. Kitipat Siemanond)

.....
(Prof. Thumrongrat Mungcharoen)

ABSTRACT

5873021063: Petroleum Technology Program

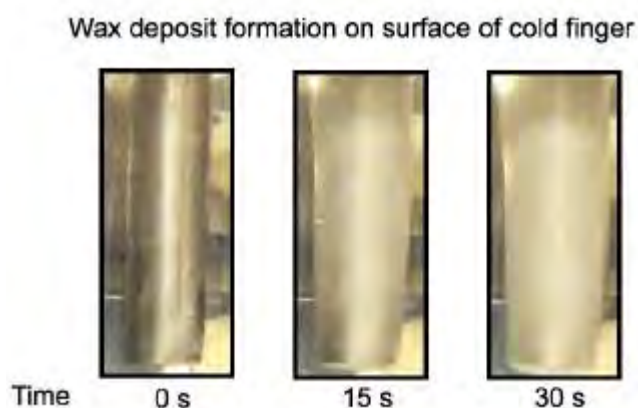
Tunya Ketjuntiwa: The Incipient Layer of wax Deposit

Thesis Advisors: Asst. Prof. Pomthong Malakul and Prof. H.Scott

Fogler 73 pp.

Keywords: Deposition/ Precipitation/ Cold finger/ Pigging/ WAT/ Reservoir/
Gelation

The formation of the incipient layer of wax deposit when waxy oil is exposed to a cold surface is studied. Using a cold-finger apparatus, the evolution of deposit thickness is monitored with a video camera, allowing one to resolve the deposit layer formation from inception up to long times where deposit thickness no longer grows. Characterization of wax deposits show that incipient layer has identical composition to waxy oil, indicating that deposit is not formed by a diffusion process. Modelling shows deposit formation at the investigated conditions cannot be explained by a diffusion process.



บทคัดย่อ

ัญญา เกษจันทร์ทิวา : การตกตะกอนชั้นของพาราฟินแว็กซ์ (The Incipient Layer of Wax Deposit) อ.ที่ปรึกษา : ผศ. ดร. ปมทอง มาลากุล และ ศ. ดร. เอช สก๊อต ฟอกเลอร์ 73 หน้า

งานวิจัยนี้จะศึกษาการเกิดระดอนของแว็กซ์ในชั้นแรก โดยตะกอนของแว็กซ์นั้นเกิดขึ้นเนื่องจากน้ำมันที่มีส่วนประกอบของแว็กซ์ถูกทำให้เย็นลง การทดลองนี้จะใช้อุปกรณ์ที่เรียกว่า cold finger วิวัฒนาการของความหนาของแว็กซ์จะถูกบันทึกโดยใช้กล้องวิดีโอซึ่งทำให้สามารถสร้างทำให้เห็นการเกิดขึ้นตะกอนของแว็กซ์ตั้งแต่เริ่มต้นจนถึงช่วงเวลาที่แว็กซ์หยุดการสร้างชั้นตะกอนลักษณะของตะกอนของแว็กซ์ที่ชั้นแรกเริ่มนั้นมีองค์ประกอบเหมือนกันกับน้ำมันที่มีส่วนประกอบของแว็กซ์ที่ใช้ในการทดลอง ซึ่งแสดงให้เห็นว่าชั้นตะกอนของแว็กซ์ที่ชั้นแรกเริ่มนั้นไม่ได้เกิดขึ้นจากกระบวนการแพร่กระจายโดยการเกิดตะกอนของแว็กซ์ในที่นี้ไม่สามารถอธิบายได้ด้วยแบบจำลองการเกิดตะกอนของการแพร่กระจาย

ACKNOWLEDGEMENTS

This thesis would not be complete without my family, my friends, my PhD and my supervisor. Firstly, I would like to say many thanks to Prof. H. Scott Fogler and Asst. Prof. Pomthong who bought this program. The visiting scholar program to the University of Michigan. Moreover, I also want to say thank you to Prof. Apanee Luengnaruemitchai who provided me suggestion about registration information for courses involved kinetic class of Asst. Prof. Pomthong. My courses registration will not accomplished without another recommendation of Asst. Prof. Manit Nithitanakul. I also feel really thankful to Asst. Prof. Kitipat Siemanond who accepts me to take my last credit course.

My first project at the University of Michigan, I started with Sheng “Mark” Zheng. It is my appreciation to work with him. Everything can be fixed and answered, he really smart person that I ever worked with. My second project, I am working with Cláudio Vilas Bôas Fávero and Luqman Hakim Bin Ahmad Mahir. It is my gratefulness to work with them. Cláudio always brought me so many new ideas about the experiments. Luqman I learn to identify information with support ideas that make things have more sense because of Luqman. I got a lot of comments from Prof. H. Scott Fogler about my slides and presentation. Because of his comments then my presentation is improved. With all of the above people, my research can move forwards.

Finally, my family that always support me. Without them, I cannot be now at this point. Moreover, I would like to thank Chulalongkorn University for the fulfillment in my master degree. I am grateful for the partial scholarship and partial funding of the thesis work provided by Petroleum and Petrochemical College.

TABLE OF CONTENTS

	PAGE
Title Page	i
Abstract (in English)	iii
Abstract (in Thai)	iv
Acknowledgements	v
Table of Contents	vi
List of Tables	xi
List of Figures	xiii

CHAPTER

I	INTRODUCTION	1
II	LITERATURE REVIEW	3
	2.1 Determination of the WAT	3
	2.2 Wax Deposition Mechanisms	3
	2.2.1 Precipitation of Dissolved Wax Molecules	4
	2.2.2 Formation of Radial Concentration Gradient	4
	2.2.3 Diffusion of Waxy Components toward Pipe Wall	4
	2.2.4 Aging of Wax Deposit	4
	2.3 Wax Deposition Experiment	5
	2.4 Effects of Operating Conditions on Wax Deposit	
	Carbon Number Distribution	7
	2.4.1 Fundamentals of Transport Modelling	
	Using the MWP	7
	2.4.2 Molecular Diffusivities of n-Alkane Molecules	
	with Different Chain Length	8

CHAPTER	PAGE
2.5 Concentration Boundary Condition at Inlet and Wall	8
2.6 The Dominant Factors in the Deposit Carbon Number Distribution	9
2.7 Designing Durable Icephobic Surface	10
2.8 Modelling Wax Diffusion in Crude Oils : The Cold Finger Device	13
2.9 Kinetic of Waxy Gel Formation	16
III EXPERIMENTAL	19
3.1 Materials	19
3.1.1 Light Mineral Oil	20
3.1.2 Paraffin Wax	20
3.1.3 Toluene	20
3.1.4 Acetone	20
3.1.5 Methyl Ethyl Ketone	20
3.2 Equipment	20
3.2.1 Cold Finger Apparatus	21
3.2.2 High Temperature Gas Chromatography	21
3.2.3 Fisher Scientific™ Plusing Vortex Mixer	22
3.2.4 Video Camera	22
3.3 Software	22
3.3.1 LabView	22
3.3.2 Microsoft Word	22
3.3.3 Microsoft Excel	22
3.4 Methodology	22

CHAPTER	PAGE
3.4.1 Prepare Oil Reservoir	22
3.4.2 Wax Deposition Cold Finger Apparatus	22
3.4.3 Cleaning Step	23
3.4.4 Finding Wax Thickness	23
3.4.5 Characterization of Wax Content by Gas Chromatography	23
IV RESULTS AND DISCUSSION	25
4.1 Assessing the Possibility of Wax Deposit Remediation With Polymeric Coating	25
4.1.1 Deposition Weight	26
4.1.2 Wax Content	27
4.2 Kinetic Study of Wax Deposition using Cold Finger Apparatus	27
4.2.1 Effect of Rpm Changes	27
4.2.2 Effect of Temperature Gradient on Deposit Formation When Changing the Jacket Temperature	28
4.2.3 Effect of Temperature Gradient on Deposit Formation When Changing the Jacket Temperature	29
4.2.4 Final Thickness of Deposit : Deposit Thickness After 2 hours of Experiment	30
4.2.5 Temperature Profile of Fluid in Vessel at Steady State	31
4.2.6 Does Deposit Stops Growing Due to Wax Depletion in Oil? Perform Mass Balance	31

CHAPTER	PAGE
4.2.7 Does Deposit Stops Growing Due to Wax Depletion in Oil? Calculation of Interface Temperature	33
4.2.8 Final Deposit Thickness and Interface Temperature Further Investigation on Final Deposit Thickness	35
4.2.9 Final Thickness and the Wax Appearance Temperature Implication 1	36
4.2.10 Final Thickness and the Wax Appearance Temperature Implication 2	37
4.2.11 Evolution of Deposit Thickness When RPM Changes	37
4.2.12 Carbon Distribution	38
4.2.13 Evolution of Deposit Thickness With Cooling Rate	39
V CONCLUSIONS AND RECOMMENDATIONS	40
REFERENCES	41
APPENDICES	42
Appendix A Calibration Curve for Finding Thickness	42
Appendix B Deposit Thickness When RPM Changes	44
Appendix C Deposit Thickness When Jacket Temperature Changes	48
Appendix D Deposit Thickness When Cold Finger Temperature Changes	50
Appendix E Thickness with Cooling Rate	52
Appendix F Thickness with 1200 PPM of PEVA	54

CHAPTER	PAGE
Appendix G Thickness When Wax Content Changes	55
Appendix H Thickness When RPM is Switched	57
Appendix I Interface Temperature, T_i by Experiment	59
Appendix J Temperature Profile by Calculation	64
Appendix K Evolution of Thickness Using Primicerio <i>et al.</i> (2006) Model	66
Appendix L Carbon Number Distribution	68
CURRICULUM VITAE	73

LIST OF TABLES

TABLE		PAGE
A1	Evolution of thickness at $T_{jac} = 45\text{ }^{\circ}\text{C}$, $\Delta T=40\text{ }^{\circ}\text{C}$, rpm=0, t= 2hr at specific time	43
B1	Evolution of thickness at $T_{jac} = 45\text{ }^{\circ}\text{C}$, $\Delta T=40\text{ }^{\circ}\text{C}$, rpm=0, t= 2hr	44
B2	Evolution of thickness at $T_{jac} = 45\text{ }^{\circ}\text{C}$, $\Delta T=40\text{ }^{\circ}\text{C}$, rpm=55, t= 2hr	45
B3	Evolution of thickness at $T_{jac} = 45\text{ }^{\circ}\text{C}$, $\Delta T=40\text{ }^{\circ}\text{C}$, rpm=135, t= 2hr	46
B4	Evolution of thickness at $T_{jac} = 45\text{ }^{\circ}\text{C}$, $\Delta T=40\text{ }^{\circ}\text{C}$, rpm=240, t= 2hr	47
C1	Evolution of thickness at $T_{jac} = 50\text{ }^{\circ}\text{C}$, $\Delta T=45\text{ }^{\circ}\text{C}$, rpm=135, t= 2hr	48
C2	Evolution of thickness at $T_{jac} = 52\text{ }^{\circ}\text{C}$, $\Delta T=47\text{ }^{\circ}\text{C}$, rpm=135, t= 2hr	49
D1	Evolution of thickness at $T_{jac} = 45\text{ }^{\circ}\text{C}$, $\Delta T=10\text{ }^{\circ}\text{C}$, rpm=135, t= 3hr	50
D2	Evolution of thickness at $T_{jac} = 45\text{ }^{\circ}\text{C}$, $\Delta T=20\text{ }^{\circ}\text{C}$, rpm=135, t= 2hr	51
D3	Evolution of thickness at $T_{jac} = 45\text{ }^{\circ}\text{C}$, $\Delta T=10\text{ }^{\circ}\text{C}$, rpm=135, t= 3hr	50
E1	Evolution of thickness at $T_{jac} = 45\text{ }^{\circ}\text{C}$, $\Delta T=40\text{ }^{\circ}\text{C}$, rpm=135, t= 3hr with cooling Rate	53
F1	Evolution of thickness at $T_{jac} = 45\text{ }^{\circ}\text{C}$, $\Delta T=40\text{ }^{\circ}\text{C}$, rpm=135, t= 2hr with 1200 PPM P-EVA	54

TABLE	PAGE
G1 Evolution of thickness 1%Wax at $T_{jac} = 45\text{ }^{\circ}\text{C}$, $\Delta T=40\text{ }^{\circ}\text{C}$, rpm=135, t= 2hr	55
G2 Evolution of thickness 2.5%Wax at $T_{jac} = 45\text{ }^{\circ}\text{C}$, $\Delta T=40\text{ }^{\circ}\text{C}$, rpm=135, t= 2hr	56
H1 Evolution of thickness $T_{jac} = 45\text{ }^{\circ}\text{C}$, $\Delta T=40\text{ }^{\circ}\text{C}$, rpm=240 1hr and rpm=0 1hr	57
H2 Evolution of thickness $T_{jac} = 45\text{ }^{\circ}\text{C}$, $\Delta T=40\text{ }^{\circ}\text{C}$, rpm=0 1.5hr and rpm=240 1.5hr	58
I1 Interface temperature $T_{jac} = 45\text{ }^{\circ}\text{C}$, $\Delta T=40\text{ }^{\circ}\text{C}$, rpm=135	59
I2 Interface temperature $T_{jac} = 45\text{ }^{\circ}\text{C}$, $\Delta T=40\text{ }^{\circ}\text{C}$, rpm=240	61
I3 Interface temperature $T_{jac} = 45\text{ }^{\circ}\text{C}$, $\Delta T=30\text{ }^{\circ}\text{C}$, rpm=135	61
I4 Interface temperature $T_{jac} = 45\text{ }^{\circ}\text{C}$, $\Delta T=10\text{ }^{\circ}\text{C}$, rpm=135	61
I5 Interface temperature $T_{jac} = 50\text{ }^{\circ}\text{C}$, $\Delta T=45\text{ }^{\circ}\text{C}$, rpm=135	62
I6 Experimental condition for finding the interface temperature	62
I7 Experimental condition for finding the interface temperature when wax content changes	63
J1 Temperature profile by calculation	64
K1 Evolution of mass by using Primicerio et al. model	66
L1 Carbon number distribution of oil before	68
L2 Carbon number distribution of oil after	69
L3 Carbon number distribution of wax deposit	70
L4 Carbon number distribution of oil before, oil after and deposit	72

LIST OF FIGURES

FIGURE		PAGE
2.1	Molecular diffusion mechanisms.	5
2.2	Cold finger schematic.	6
2.3	Bulk and wall temperature differences for different n-alkane components.	9
2.4	Half-coated license plate during outdoor winter 2013.	11
2.5	Temperature profile across the cold finger apparatus.	12
2.6	Deposit as function of time.	13
2.7	Heat transfer at cold finger wall.	15
3.1a	Composition of wax in paraffin wax.	16
3.1b	Composition of wax mineral oil.	19
3.2	Schematic of cold finger apparatus.	19
3.3	Michigan cold finger apparatus.	20
3.4	Michigan Gas chromatography.	21
3.5	Experimental procedure flow chart.	21
3.6	Finding wax deposit thickness.	24
4.1	Deposit from cold finger experiment.	24
4.2	Deposit weight from cold finger experiment in graph.	25
4.3	Wax content from cold finger experiment.	26
4.4	Thickness vs time when varies rpm.	26
4.5	Thickness vs time when varies T_{jac} .	28
4.6	Deposit weight vs time at varies T_{cf} .	29
4.7	Final deposit thickness.	30
4.8	Temperature profile across cold finger.	31

FIGURE	PAGE
4.9 Find the mass balance in oil before, oil after and wax deposit.	32
4.10a Oil before and oil after wax composition.	32
4.10b WAT of oil before and oil after.	32
4.11 Heat transfer across sold finger apparatus.	34
4.12 Interface temperature.	34
4.13 Resistances across cold finger.	35
4.14 Temperature profile when WAT increases.	36
4.15 Final wax deposit thickness when wax content increases.	37
4.16 Final wax deposit thickness when rpm changes.	37
4.17 Wax deposit thickness when rpm changes.	38
4.18 Final wax deposit thickness when rpm changes.	39
4.19 Carbon distribution.	39
A1 Calibration curve.	42
A2 Comparison of calculated mass vs measured mass.	42
A3 The error between calculated mass and measured mass.	43
E1 Cooling rate.	52
I1 Interface temperature.	62
I2 Interface temperature when wax content changes.	63
J1 Temperature profile by calculation $T_{jac} = 45\text{ }^{\circ}\text{C}$, $\Delta T=40^{\circ}\text{C}$, rpm=240.	65
K1 Evolution of mass by Primicrio <i>et al.</i> (2006) model. Carbon number distribution of oil before, oil after and deposit.	67
L1 Carbon number distribution of oil before, oil after and deposit.	71
L2 Mass balance of oil before, oil after and deposit.	72

CHAPTER I

INTRODUCTION

One of the most important problems in oil and gas industry is wax deposition. Wax deposition can happen in various locations during operation since production, transportation and storage. Crude oil is a mixture of waxes, aromatics, naphthenes, asphaltenes and resins (Huang *et al.*, 2011). Moreover, waxy component in crude oil referred to carbon numbers greater than 20 (Lee, 2008). It represent a group of n-alkanes which known as n-paraffins.

One of very specific problem of waxy crude oil is wax deposition during transportation. At reservoir condition which is relatively high temperature, waxes are dissolved in crude oil. However, during oil transportation from reservoir to any processing facilities, its temperature is reduced continuously. Moreover, when the temperature fall below appearance temperature (WAT) (Berne Allen and Work, 1938), waxy components will start to precipitate out of the crude oil and form solid layer. This solid waxy layer can decrease ability of crude oil flowing through pipeline, causing reduction in oil production. In addition, pressure drop will increase and can cause safety issue.

There are some methods that have been used, in order to minimize this problem. Firstly, pipeline insulation but, this solution could increase a lot of production cost. Secondly, is most the common technique that applied for long distance which is called “pigging”, the inspection gauge or “pig” is sent in the pipeline to scrape off the wax deposits on the wall (Huang *et al.*, 2011). However, production needs to stop while doing pigging. Therefore, this method also can increase the production cost.

In this study, there are two main research topics. The first one is Assessing the possibility of wax deposit remediation with polymeric coating which is the previous topic that proposed in proposal. However, the result that found at the end does not meet the expectation which will be disused in the result and discussion section. As the result, next topic which is the title of this report “Kinetic study of wax deposition using cold finger apparatus” has been studied.

In the first study, a new method is proposed. As Professor Anish Tuteja at the University of Michigan have created surfaces that are able to prevent adhesion of ice. Because of that, the new ideas that these novel surfaces can potentially also be used to prevent adhesion of wax is presented. The purpose of this study is to explore the applicability of polymeric coating for the remediation of wax deposit by reducing wax adhesive. The experiment was performed in the cold finger experiment. The deposit weight and wax content was measured and compared between the bare stainless steel cold finger and cold finger with coating material.

In the second study, as cold finger is immersed into the reservoir or jacket, there is a layer of deposit form immediately. There could be because of another step of wax deposition called “gelation” involved in the wax mechanism which occurred by temperature gradient between bulk hot fluid in the reservoir and cold surface of cold finger. There was no experiment that has been done in the cold finger apparatus and showed this phenomenon before. If this spectacle can be explained by this experiment, it could change the wax mechanism that has been suggested before. The purpose of this study is to determine the process of wax deposition when gelation dominates the process. The technique of video recording is introduced while experiment is running, in order to see the changed since the beginning of experiment. The thickness could be determined from the video. Moreover, deposit sample is collected to measure the weight and analyzed by the HTGC to find the carbon distribution of each sample.

CHAPTER II

LITERATURE REVIEW

2.1 Determination of the WAT

WAT stands for Wax Appearance Temperature which is the temperature that wax starts to precipitate from crude oil. It also known as cloud point temperature. WAT is one of the most important parameter when designing any processes in oil and gas industry. Moreover, with different sources of crude oil, compositions in crude oil are varied hence, WAT is changing. There are many methods to measure the WAT such as visual inspection, CPM Techniques, Fourier-Transform Infrared Spectroscopy (FT-IR), Viscometry and Thermal Techniques (DSC).

2.2 Wax Deposition Mechanisms

Wax deposition mechanisms eventually proposed by Burger, Perkins, and Striegler (1981). There are molecular diffusion, shear dispersion, Brownian diffusion and gravity settling. However, the main mechanisms for wax deposition is molecular diffusion, as the another mechanisms have insignificant impact on wax deposition.

Molecular diffusion involved of 4 steps which are Precipitation of dissolved wax molecules, Formation of radial concentration gradient, and Diffusion of waxy components toward pipe wall and Aging of wax deposit.

2.2.1 Precipitation of Dissolved Wax Molecules

When crude oil temperature is decreased to below the wax appearance temperature (WAT), waxy components that originally dissolved in oil start to precipitate out of the oil and form solid crystal. Precipitation can take place both at bulk fluid and pipe wall. However, just waxy components that precipitated in pipe wall form the incipient layer of the wax deposition. The precipitated waxy components at bulk fluid, will flow with oil and not form deposition layer.

2.2.2 Formation of Radial Concentration Gradient

There is a radial concentration gradient between bulk oil and pipe wall because usually wall temperature is less than bulk oil. As the result, precipitated waxy component at the wall is greater than in the bulk oil. The waxy components in bulk oil then move toward the wall and precipitate.

2.2.3 Diffusion of Waxy Components Toward Pipe Wall

The wax deposition occurs because of the accumulated waxy components that precipitated on the wall. When, precipitation proceeds, wax deposit will get thicker. Furthermore, with fluid continues flowing through the pipe; waxy components which have carbon number greater than critical carbon number (CCN) (Singh *et al.* 2000) then continue move toward the pipe wall and wax deposit is being built up.

2.2.4 Aging of Wax Deposit

Above the solubility limit, further precipitation does not form a new layer of deposit. Waxy components that continue diffuse into deposit will just increase the wax fraction of deposit. In addition, waxy components in deposit those have carbon numbers lower than critical carbon number (CCN) will counter-diffusion away from surface (Singh *et al.*, 2000) which made deposit getting harder. This process is called deposit aging.

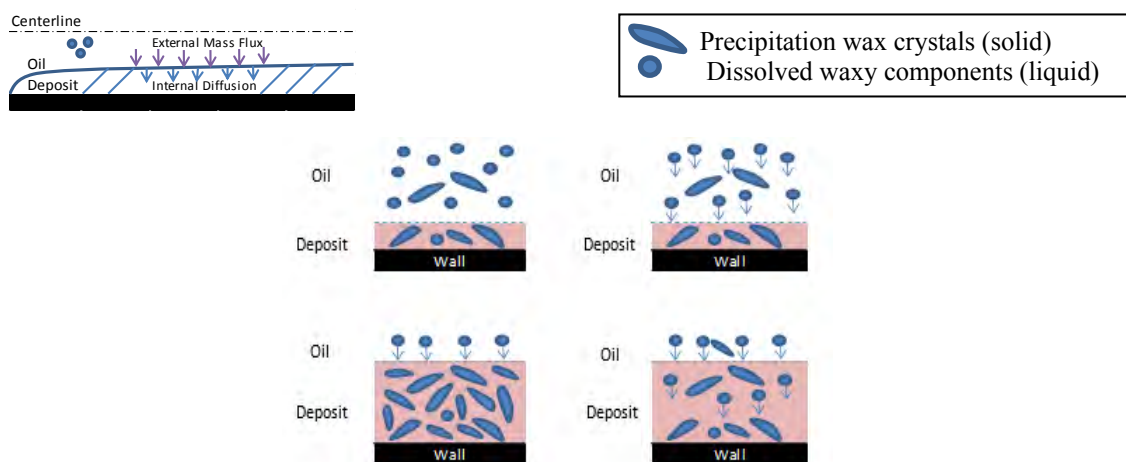


Figure 2.1 Molecular diffusion mechanisms.

2.3 Wax Deposition Experiment

The objective of modeling the wax deposition is to get the predicted wax properties for example thickness, composition and wax content. As the result, they can be applied to the field operation. In pipeline, we will be able to know how often, we need to send the “pig” into the pipeline. A “pig” is an instrument that sent into pipeline, in order to clean the pipeline and this process is called pigging. Because of high frequency in pigging will increase more operation cost. In another word, we can save a lot of money by knowing the predicted wax thickness. In the University of Michigan lab, there are two main apparatuses that have been performed to study the wax deposition which are “Flow Loop” and “Cold Finger”.

Flow loop is the most expensive wax deposition apparatus and it also the best experimental tool for wax deposition modeling. (Creek *et al.*, 1999; Hernandez, 2002; Hoffmann and Amundsen, 2010). Flow loop has a test section which similar to field pipeline, then by scale-up from flow loop tends to give the most consistent result for wax deposition. However, flow loop apparatus is also the most complex experiment, because it contains of several parts: conditioning system, pumping system, test section and deposit characterization device (Huang *et al.*, 2015).

Cold finger is less expensive than flow loop and it is a smaller unit experiment. Cold finger requires fewer amounts of oil and wax. There are two main components of a cold finger apparatus, the deposit cell and the circulation system (Huang *et al.*, 2015).

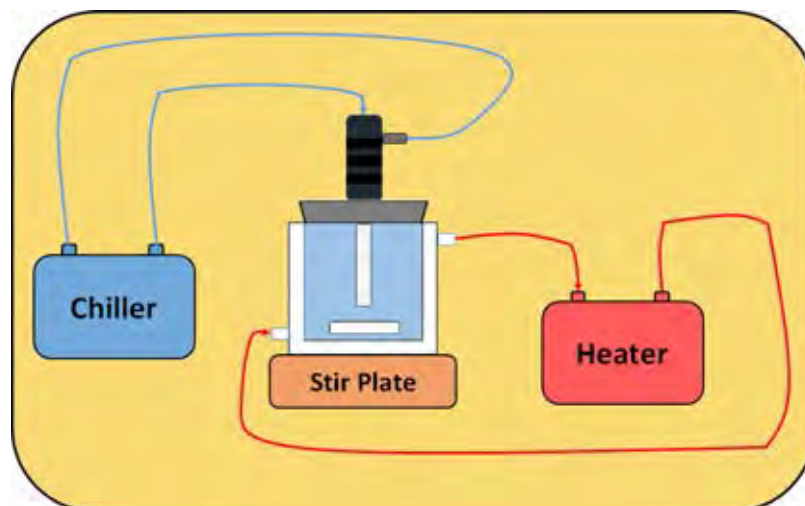


Figure 2.2 Cold finger schematic.

Figure 2.2, shows a schematic diagram of a cold finger in the University of Michigan laboratory. The deposition cell includes a stainless steel cylinder which is a cold finger probe. Cold finger is maintained to be at low temperature, then wax will deposit on its surface (Huang *et al.*, 2015). During the wax deposition a cold finger probe is placed inside the jacket. The stir bar is put in the container or jacket, in order to introduce shear force to the system. Shear level can be adjusted by the speed button on the heat plate. The circulation system includes a heating system and cooling system. Reservoir or jacket needs high temperature, more than WAT. It provided energy from the heater. In another hand, cold finger probe should set to the temperature below WAT, which is adjusted by Chiller. After running, the deposit on cold finger probe might contain some residual oil which needs to remove by methyl ethyl ketone, MEK. Cold finger probe is dipped to MEK solution before collecting the sample. The deposit will collected to measure the weight by scale and measure wax content by GC, Gas Chromatography.

2.4 Effects of Operating Conditions on Wax Deposit Carbon Number Distribution

2.4.1 Fundamentals of Transport Modelling Using the MWP

Both heat and mass transport modeling are involved in thermodynamic modeling in order to identify the carbon number distribution in of wax deposits. It has been found that the carbon distribution is associated with different n-alkane components diffusion and also their concentration driving force.

Fundamental of transport modeling used by MWP combine with Coutinho's thermodynamic model is developed to model mass transfer of wax from the liquid bulk toward the wall. The fundamental transport and boundary conditions are shown in equation1 and equation2 respectively.

$$V \frac{\partial C}{\partial z} = \frac{1}{r} \frac{\partial}{\partial r} [(\epsilon_{mass} + D_{wo}) r \frac{\partial C}{\partial r}] \quad (1)$$

V is the velocity of the fluid, C is the concentration of wax in liquid phase, z is the axial position, r is the radial position, D_{wo} is the diffusivity of wax in oil, and ϵ_{mass} is the eddy diffusivity.

$$\text{At } z = 0, C = C_{inlet} \quad (2)$$

$$\text{At } r = 0, \frac{\partial C}{\partial r} = 0 \quad (3)$$

$$\text{At } r = R, C = C_{interface} \quad (4)$$

2.4.2 Molecular Diffusivities of n-Alkane Molecules with Different Chain Length

As the difference in molecular size, the difference in diffusivities while modeling of molecular diffusion of multiple components needs to be considered. The molecular diffusivity decreases when the carbon chain length increases because of the bulkiness of the molecules increased. MWP uses the Hayduk-Minhas equation to calculate the diffusivity of n-alkanes which shown below.

$$D_{wo,i} = 13.3 \times 10^{-12} \frac{T^{1.47} \mu^{\left(\frac{10.2}{V_{A,i}} - 0.791\right)}}{V_{A,i}^{0.71}} \quad (5)$$

$D_{wo,i}$ is the molecular diffusivity of wax in oil, T is the temperature of fluid, μ is the viscosity of the fluid, and $V_{A,i}$ is the molar volume of the diffusing n-alkane.

2.5 Concentration Boundary Condition at Inlet and Wall

The n-paraffin species at the inlet and wall can be assumed to be in the thermodynamic equilibrium at the inlet and wall temperature respectively. Moreover, the particular n-paraffin concentration depends on the amount of n-C_iH_{2i+2} in crude oil and its solubility at the particular temperature. As the result, the concentration of n-alkane component at inlet and wall need to be specified individually by Coutinho's thermodynamics model. However, it should be noted that the branched-cyclic components did not included in thermodynamic modeling because they does not precipitate as their melting point less than their isomers with the same carbon number. In another hand, the non-normal n-paraffins usually do not precipitate because they have melting point higher than the n-paraffin with the same carbon number. Furthermore, the n-paraffin species with carbon numbers lower than 15 also do not precipitate as their melting point less than 5°C.

The Coutinho's model needs the crude oil composition as the input parameter. The composition can be divided into two groups, the single carbon number and n-paraffin distribution. The single carbon number (SCN) includes, branched paraffin, cyclic paraffin, aromatics and n-paraffin with carbon number i. So, the molecular formula of the components in SCN with carbon number i can be written as C_iH_j, where j = 2i+2 represents paraffinic components and j ≠ 2i+2 represents aromatics. Besides, the n-paraffin distribution included only n-paraffin.

From the experiment of Zheng *et al.* (2013), it can be concluded that at the particular temperature Coutinho's model can precisely predict the total amount of precipitation as the result from the model and HTGC gave the same trend. There are two trends that can be detected. Firstly, At the certain temperature, the weight fraction of n-C_iH_{2i+2} first increases, reaches a maximum then decreases. Secondly,

the peak of carbon distribution shifts toward greater carbon number as the temperature increased.

2.6 The Dominant Factors in the Deposit Carbon Number Distribution

As the different in mass flux causes the carbon number distribution in deposit, the component with larger mass fluxes are expected to be more enhanced in the deposit than the lower mass fluxes component. Moreover, the main factor that affects the mass flux is a concentration driving force. There is a term “Critical carbon number, CCN” which is the carbon number that point out whether the diffusion is moving toward the wall or away of wall. When carbon number i less than CCN, it means that the concentration of bulk fluid less than the wall. So, the molecule moves away from wall. In another hand, as carbon number i greater than CCN, the bulk fluid concentration is greater than wall concentration then the carbon molecule moves forward the wall.

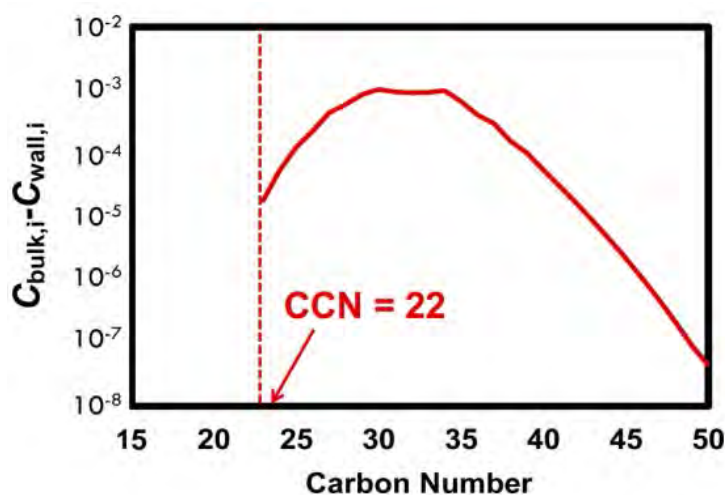


Figure 2.3 Bulk and wall temperature differences for different n-alkane components (Zheng *et al.*, 2013).

In Figure 2.3, it can be seen that the concentration driving force increases at first as carbon number increases, after that it drops down from the maximum point. In this case CNN is 22. The reason which these phenomena happened is that as i increases, the solubility of $n\text{-C}_i\text{H}_{2i+2}$ increased then the wall concentration declined. As the result, the different in concentration is bigger. However, as i increase, the concentration of bulk fluid also decreases because the oil contains less $n\text{-C}_i\text{H}_{2i+2}$ which cause the curve then falls down from peak.

From the flow loop experiment, it can be concluded that even when the conditions are changed, but if keep the normalized distribution the same. The carbon distribution of wax deposit is nearly the same. Normalized distribution, ΔC can be calculated by dividing each concentration ΔC_i by the sum of all the concentration driving force, $\sum \Delta C_i$. In another hand, when the conditions are changed and different in normalized distribution. It can be found that as the coolant temperature or oil volumetric flow rate decreased which effect to the decreasing in wall temperature. As the result, carbon distribution trend to shift to the small carbon number. The reason is that as the temperature decreased small carbon number can deposit more on the surface.

2.7 Designing Durable Icephobic Surface

Professor Anish Tuteja from department of Material Science at the University of Michigan has studied about the icephobic surfaces. Icephobic surfaces are defined as the surfaces that have an ice adhesion strength less than 100 kPa. ($\tau_{\text{ice}} < 100 \text{ kPa}$). Currently, the lowest ice adhesion values made from the material of lubricants or gels. Lubricated reduces the ice adhesion by minimizing the contact angle hysteresis on the surface through the formation of low surface energy lubricating free-oil layer (Tuteja *et al.*, 2016). However, there is an advantage as it has short-lived because oil can be removed by water droplet of frost.

Professor Tuteja then has studies about ice adhesion properties of Elastomers. Elastomers have a property in between of liquid and solid. The viscoelastic of elastomers is controlled in two ways. Firstly, the adhesion strength is reduced by diminishing the cross link density, ρ^{CL} which made the elastomer softer.

For example, polydimethylsiloxane (PDMS) with a lot of cross-links has ice-adhesion strength of over 250kPa, whereas PDMS with fewer cross-links has adhesion strength of just 33kPa. Due to, the stress required to shear two surfaces apart is direct proportion to cross link density, which happen through interfacial cavitation process. Secondly, adding the ability of interfacial slippage or oil to Elastomer can help to achieve very low ice adhesion. The relation between ρ^{CL} and τ_{ice} with no interfacial slippage is $\tau_{ice} \propto \rho^{CL1/2}$ and with the interfacial slippage is $\tau_{ice} \propto \rho^{CL}$.

Figure 2.4, is one of the evidence that the polymeric coating can use to prevent the ice deposition during winter from ice storm. Half of the plate is coated by PDMS and placed outside during the night. Follow by the next day morning, the plate was imaged. The uncoated side significant showed ice accretion, whereas coated side had no ice at all.

As the result, Fogler's group has an idea that with coating material maybe can help to reduce the wax deposition. Then the experiment will perform with cold finger both coated cold fingers and uncoated cold finger in order to see the different between in wax deposition. The cold fingers are coated by Professor Tuteja team.



Figure 2.4 Half-coated license plate during outdoor winter 2013 (Tuteja *et al.*, 2016).

2.8 Modelling Wax Diffusion in Crude Oils : The Cold Finger Device

Wax diffusivity and solubility values in crude oils from deposition measurements in the cold finger with stirring. (Primicerio *et al.*, 2006) The experiment is done under cold flow condition which oil temperature or heater less than WAT as well as cold finger temperature. The mixer is placed at the bottom as to provide the simultaneously shear. It has been observed that in the case of no stirring, the system evolves through three stages: (i) complete saturation, (ii) partial desaturation, (iii) complete desaturation. In the stirred case, because of homogenization, stage two does not exist and the system evolves from complete saturation to complete desaturation. (Primicerio *et al.*, 2006) The following assumptions are satisfied in this conceptual model.

- Deposition is due only to molecular diffusion
- The saturation concentration C_s (solubility) is a linear function of temperature T.
- Oil and wax have the same constant density ρ (typically 800 kg/m^3)

Denote that: C_{tot} is total wax concentration

C_{tot}^* is initial total wax concentration

c is dissolved wax concentration

G is segregated wax concentration

C_{cloud} is cloud point

Under the assumption that thermo dynamical equilibrium between dissolved and segregated phase is instantaneously we will get,

$$C_{tot} = c + G \quad (6)$$

$$G = [c - C_s(T)] \quad (7)$$

$$C_{tot}^* = C_s(T_{cloud}) \quad (8)$$

The Mathematical Model

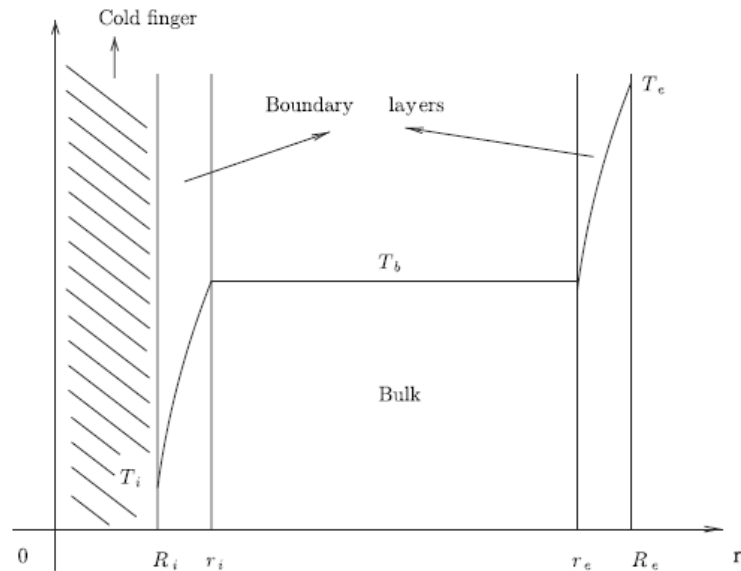


Figure 2.5 Temperature profile across the cold finger apparatus (Primicerio *et al.*, 2006).

The bulk zone is at constant temperature, T_b . In the first stage the deposition rate is constant and mass grows linearly with time. In the second stage the deposition rate tends asymptotically to zero (exponential decay). Mass diffusion takes place in the boundary layer near the cold wall, where a thermal gradient is present. As long as the bulk remains saturated the loss of wax due to deposition is balanced by dissolution of segregated bulk tends to the saturation is achieved the deposition rate starts to decrease and the wax concentration in the bulk trends to the saturation concentration corresponding to the cold finger temperature. The deposit is formed by oil and wax fraction ϕ is assumed to be independent of time. The value of ϕ is expected to be larger than in the static device and closer to the ones found in pipeline deposits. (Primicerio *et al.*, 2006)

From Figure 2.5, temperature across cold finger can be calculated using equation 9 through equation 16.

$$T(r) = T_i + \frac{T_b - T_i}{\ln\left(\frac{r_i}{R_i}\right)} \ln\left(\frac{r}{R_i}\right), R_i \leq r \leq r_i \quad (9)$$

$$T(r) = T_e + \frac{T_b - T_e}{\ln\left(\frac{r}{R_e}\right)} \ln\left(\frac{r}{R_e}\right), R_e \leq r \leq r_e \quad (10)$$

T_i is cold finger temperature, K

T_b is bulk temperature, K

T_e is jacket temperature, K

r is radius at from center of cold finger at specific location, m

R_i is outer radius of cold finger, m

r_i is a boundary layer from cold finger, m

R_e is outer radius of Jacket, m

r_e is a boundary layer from Jacket, m

At the boundary layer $R_i \leq r \leq r_i$,

$$q_i = 2\pi R_i h (T_b - T_i) \quad (11)$$

q_i is a Heat flux per unit height, W/m^2

h is heat transfer coefficient, $W/m^2 \cdot K$

And, temperature profile at $R_i \leq r \leq r_i$ can be found using equation 12

$$\frac{dT}{dr}(R_i) = \frac{T_b - T_i}{\ln\left(\frac{r_i}{R_i}\right)} \frac{1}{R_i} \quad (12)$$

$$r_i = R_i \exp\left\{\frac{k}{h_i R_i}\right\} \quad (13)$$

$$r_e = R_i \exp\left\{\frac{k}{h_e R_e}\right\} \quad (14)$$

k is thermal conductivity, $W/m \cdot K$

$$h = \frac{k}{R_i^2 - m} \left(\frac{\rho \omega (R_e - R_i)}{2\mu}\right) m \quad (15)$$

ω is rotational speed, rpm

μ is viscosity, Pa.Sec

m equals to 0.628

We obtain,

$$T_b = \frac{R_e T_e + R_i T_i}{R_e + R_i} \quad (16)$$

T_b is bulk temperature, K

After we know temperature profile across the cold finger, we can find mass of wax deposited by follow equation 17 to 20.

$$b_w = \frac{[m_{w\infty}^2 - m_{w0}^2] 2R_i}{(R_e^2 - R_i^2)(\Delta T^2 - \Delta T^2)} \quad (17)$$

$m_{w\infty}^1$ is dissolved wax concentration at cold finger temperature T_1 , K

$m_{w\infty}^2$ is dissolved wax concentration at cold finger temperature T_2 , K

b_w is a fraction that obtained using asymptotic mass measurement

$$m_w(t_o) = \frac{b_w(T_{cloud} - T_b)(R_g^2 - R_i^2)}{2R_i} \quad (18)$$

m_w is deposited wax mass per unit surface, kg/m^2

t_o is desaturation time, sec

T_{cloud} is cloud point temperature, K

$$D_w = \frac{m_w^* k}{t^* b_w h \Delta T} \quad (19)$$

D_w is wax diffusivity m^2/sec

m_w^* is a measured deposited wax at time t^*

$$m_w(t) = m_w(t_o) + \frac{b_w(R_g^2 - R_{cf}^2)(T_b - T_i)}{2R_{cf}} \left[1 - \exp\left(-\frac{2D_w h R_{cf}}{k(R_g^2 - R_{cf}^2)}(t - t_o)\right) \right] \quad (20)$$

R_{cf} is a cold finger radius, m

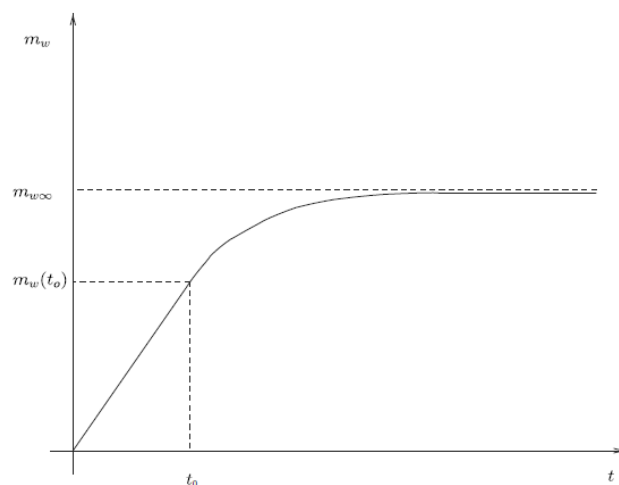


Figure 2.6 Deposit as function of time (Primicerio *et al.*, 2006).

Figure 2.6, represents the result that calculated using equation from 9 to 20. It is a deposit mass per surface area as a function time.

2.9 Kinetic of Waxy Gel Formation

The wax mechanisms that mentioned section 2.2 may not fully understood. The wax mechanisms through molecular diffusion is a step that focus on the radial transportation to the cold surface. However, from the experiment evidence, the important role may be played by axial convective transport and the oil gelation on the cold surface. Gelation is faster than molecular diffusion and may lead to the formation of a loose solid network that is slowly filled by diffusion and aging in a successive step. (Daniel *et al*, 2006.)

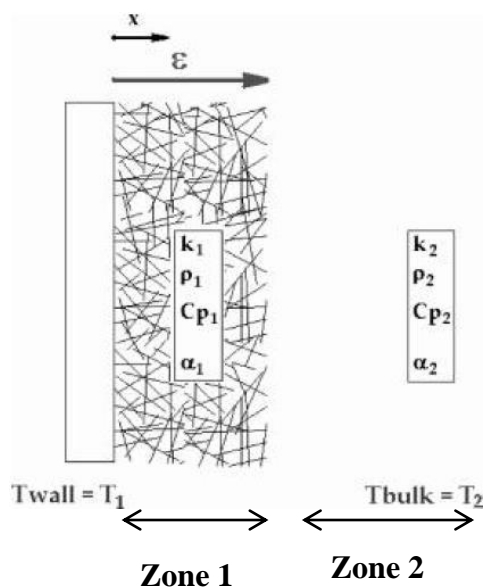


Figure 2.7 Heat transfer at cold finger wall (Daniel *et al.*, 2006).

From Figure 2.7, gelation is divided into two zones: zone 1, where the waxes have already solidified, and zone 2, where there is only liquid. (Daniel *et al.*, 2006.)

The following equation holds for the transfer of heat in zone 1:

$$\frac{\partial T_1}{\partial t} = \alpha_1 \nabla^2 T_1 - \frac{k_1}{\rho_1 \lambda} \left(\frac{\partial f}{\partial t} \right) \nabla^2 T_1 \quad (21)$$

α is the thermal diffusivity. T_1 is temperature at zone1. t is time. k_1 and ρ_1 are the thermal conductivity and the density of the deposit, respectively. λ is the latent heat of solidification and f is the fraction of solidified waxes.

The following equation holds for the transfer of heat in zone 2:

$$\frac{\partial T_2}{\partial t} = \alpha_2 \nabla^2 T_2 \quad (22)$$

α is the thermal diffusivity. T_2 is temperature at zone2 and t is time.

The initial conditions:

$$\varepsilon = 0 \text{ at } t=0 \quad (23)$$

$$T_2 = T_o \text{ at } t = 0 \quad (24)$$

ε is thickness

The boundary conditions are as follows:

$$T_1 = T_{wall} \text{ at position } 0 \quad (25)$$

$$T_1 = T_2 = T_{WAT} \text{ at the interface } \varepsilon \quad (26)$$

$$(k_1 \nabla T_1 - k_2 \nabla T_2)_\varepsilon = \rho_1 \lambda \frac{d\varepsilon}{dt} \quad (27)$$

Equation 11 states that interfacial temperature equals to WAT all the time by suggestion of Bhat and Mehrotra. In spite, in Herein experiment demonstrates that bulk temperature is decreasing by time even below the WAT. Therefore, equation 11 is just an assumption. The gelation occurred because of the difference between heat transfer in zone1 and zone2. (Daniel *et al.*, 2006.) From all of the above equation the thickness ε can be calculated by the following equation:

$$\varepsilon = bt^{0.5} \quad (13)$$

Where b can estimate by:

$$\frac{\sqrt{\pi}}{2} b \lambda \rho_1 = \frac{k_1 T_{wall} \exp(-\frac{b^2}{4\alpha_1})}{(\alpha_1)^{0.5} \operatorname{erf}(\frac{b}{2(\alpha_1)^{0.5}})} + \frac{k_2 T_o \exp(-\frac{b^2}{4\alpha_2})}{(\alpha_2)^{0.5} \operatorname{erf}(\frac{b}{2(\alpha_2)^{0.5}})} \quad (28)$$

However, the thickness rate that found from above equation just valid for the initial thickness rate as it considers that temperature of liquid (zone2) is always constant.

Daniel mentioned that, there are three processes in wax mechanisms which are:

- Deposit growth by gelation. It is a fast process than molecular diffusion.
- The deposit thickness stabilized either due to the interfacial temperature reach WAT or shear stress on the interface becomes larger than resistance of the solid network.
- Aging by radial diffusion. This step is the same as in section 2.2.4. It is a slow process. The concentration of deposit increase due to temperature gradient.

Moreover, Daniel also pointed out two variables which are WAT and Pour point (PP). Pour point is the temperature that liquid losses its flow character. From the experiment, when initial fluid temperature higher than WAT and wall temperature higher than WAT, there is no deposit on the wall. As the wall temperature reduced lower than WAT but higher than PP, there is smaller deposit when compared to wall temperature less than PP. As the result, it can be seen that it can be explained that PP is just the parameter that depresses the capability of wax deposit on the wall. It is not the parameter that determines whether there is deposit or not.

CHAPTER III EXPERIMENTAL

3.1 Materials

3.1.1 Light Mineral Oil (Crystal Plus 70T from STE Oil Company)

Mineral oil was used as a major component in model oil.

3.1.2 Paraffin Wax (m.p. $\geq 65^{\circ}\text{C}$)

5.0 wt. % of light wax in oil was added in mineral oil as wax reservoir in model oil.

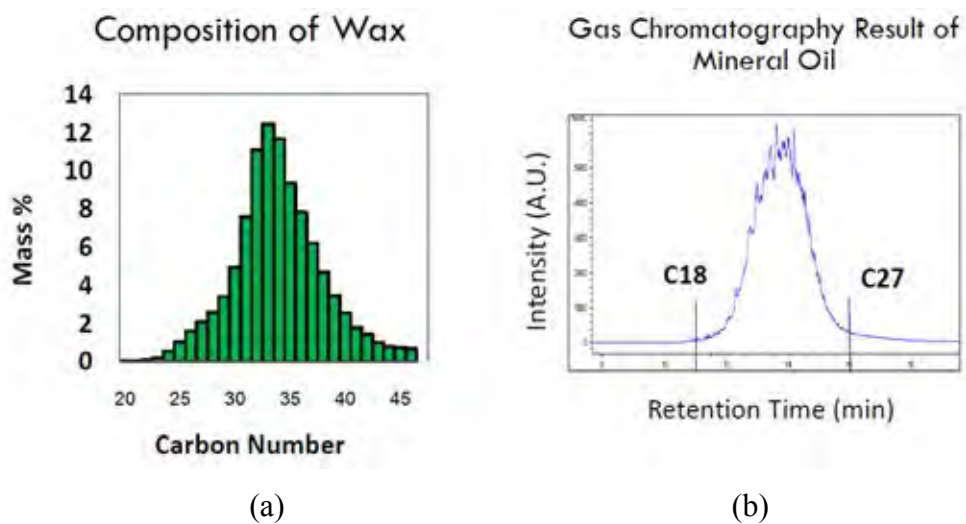


Figure 3.1 (a) Composition of wax in paraffin wax (b) composition of wax in mineral oil.

3.1.3 Toluene

99.9% pure toluene (HPLC grade) was used as a solvent for HTGC analysis and for cleaning the system after finish the experiment.

3.1.4 Acetone

99.97% pure acetone (HPLC grade) was used to clean the system after finish the experiment.

3.1.5 Methyl Ethyl Ketone

3.2 Equipment

3.2.1 Cold Finger Apparatus

The cold finger experiment was conducted to first screen the possibility of wax deposition on any desired condition. The schematic of cold finger apparatus is shown in Figure 3.2. The temperature of oil phase was controlled by the jacket reactor which has water as heating media. The temperature of the cold finger surface was kept control using coolant flow. Once the desired set points were reached, the cold finger surface was dipped into mixture in jacketed reactor. Wax deposition was started to occur at the cold finger. Figure 3.3 shows the cold finger apparatus in Michigan Laboratory when melting waxes in mineral oil.

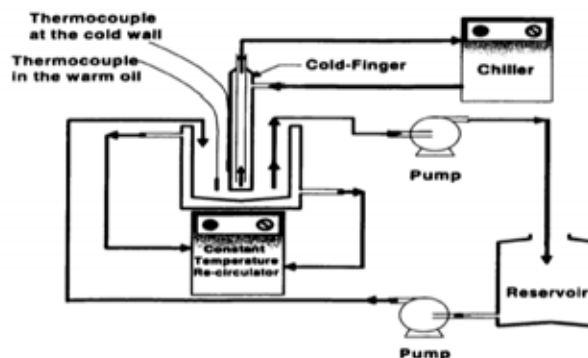


Figure 3.2 Schematic of cold finger apparatus (Singh, 2000).



Figure 3.3 Michigan cold finger apparatus.

3.2.2 High Temperature Gas Chromatography

The wax content in the deposit was determined using a Hewlett-Packard 6890 GC equipped with a capillary column coated with HP-5 (30 m x 0.320 mm x 0.25 μ m). The oven temperature was initiated at 50°C and increased to 350°C at a rate of 15°C/min and then maintained at 350°C for 20 minutes. The sample was diluted with toluene. It was centrifuged at 14000 rpm for 5 min. Then, supernatant is taken and diluted 100 times. After dilution 4 drops of sample with 3.8 ml of toluene then inject the solution into GC. The peaks of normal paraffin data were integrated on chromatogram to calculate the wax content.



Figure 3.4 Michigan Gas chromatography (Singh, 2000).

3.2.3 Fisher Scientific™ Plusing Vortex Mixer

3.2.4 Video Camera

3.3 Software

3.3.1 Lab View

3.3.2 Microsoft Word

3.3.3 Microsoft Excel

3.4 Methodology

3.4.1 Prepare Oil Reservoir

Firstly, tare the watch dish with a weighing paper on top by the scale. Then weight out 5% of wax which is 9.923g and place the wax in the reservoir jacket. Follow by, measure out the 220 ml. of oil with a measuring cylinder and pour into the reservoir.

3.4.2 Wax Deposition Cold Finger Apparatus

After sample has prepares, fixate the jacket with the chain. Then connect the two tubes between reservoir and chiller. Before open the chiller, make sure that that water in chiller tank is at an appropriate level (between high and low). Turn on the chiller and set the temperature to 60 °C and turn on the magnetic stir at level 3 and wait until wax is completely dissolved. For the cold finger side, turn on cold finger water bath and set the cold finger temperature to desire temperature. In this experiment, cold finger temperature is desired to be 5 °C. After entirely wax dissolved, adjust the temperature to the desire reservoir temperature. For this experiment, reservoir temperature is desired to be 45 °C. Wait until reservoir and cold finger temperature reaches the set point. Put cold finger in jacket and wait for wax deposit to form and grow. Wait until the time achieves to the desired time for

wax deposition. After the time is reached, take off the cold finger out from the reservoir then wash the wax deposition on cold finger with MEK. Tare the container for collecting deposit on the scale. Collect the cold finger deposit in prepared container and weight the amount of wax deposition on cold finger by scale.

3.4.3 Cleaning Step

After the experiment is done, take off two tubes between the chiller and the cooling jacket and take off the chain that around the jacket. Empty the water in the cooling jacket and Pick the stir bar from jacket with a plier. Pour the model oil in the reservoir into the waste container. Wash the reservoir and a stir bar with detergent and water, dry the reservoir. Wash the uncoated cold finger with Toluene and Acetone. For the coated cold finger, heat it up to 50 °C and let the deposit come off in the breaker.

3.4.4 Finding Wax Thickness

Video was recording entire the experiment, so the evolution of thickness can be measured. However, in order to start finding thickness from the video, the calibration curve needs to be established. After that we can start use the calibration curve to find actual thickness of wax deposit on the cold finger. When we have a diagram of wax deposit at the specific time, we first adjust the image to 3.48 inches that represented in a blue line in Figure 3.5. Secondly, draw a red line equals to the deposit thickness and lastly, use the calibration curve to find the actual wax deposit thickness. So, the evolution of thickness is obtained. (See Appendix A)

3.4.5 Characterization of Wax Content by Gas Chromatography

The wax content in the deposit was determined using a Hewlett-Packard 6890 GC equipped. The initial temperature is at 50°C and increased to 350°C at a rate of 15°C/min and then maintained at 350°C for 20 minutes. The sample is prepared by diluting with toluene in order to get the concentration around 0.284 weight percent. Then inject 1.8 microliter of sample into HTGC. HTGC will give the carbon distribution of deposit, and then from integrating peak of normal paraffin, wax content can be calculated.

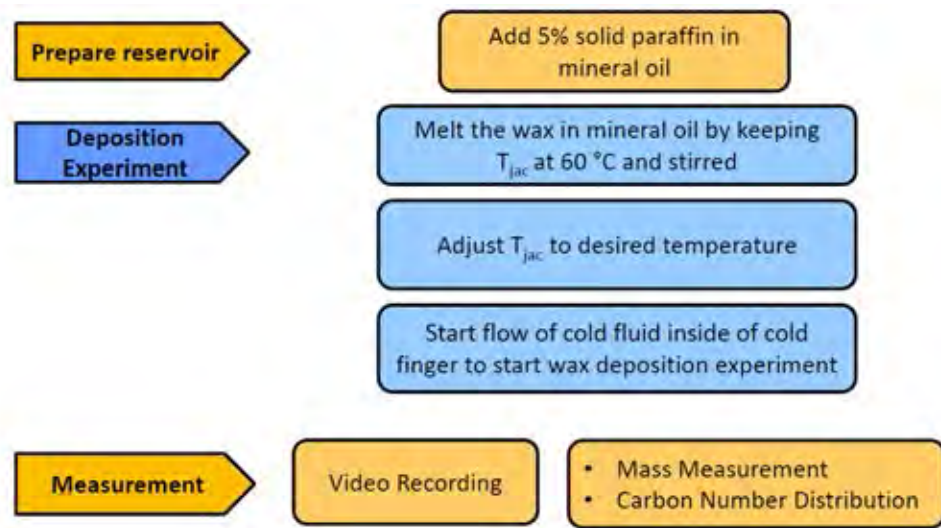


Figure 3.5 Experimental procedure flow chart.

Figure 3.4 represents experimental flow chart which explained in 3.4.1 to 3.4.5.

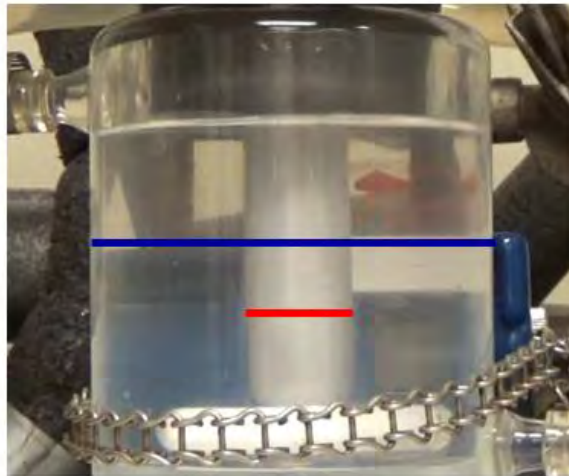


Figure 3.6 Finding wax deposit thickness.

CHAPTER IV

RESULTS AND DISCUSSION

4.1 Assessing the Possibility of Wax Deposit Remediation with Polymeric Coating

4.1.1 Deposition Weight

There are two cold fingers that coated from Kevin Golovin, a PhD student of Professor Tuteja's lab. The first one is coated by polyurethane rubber and the second one is coated by silicone (PDMS) rubber. It is referred by coating1 and coated2 respectively. There are 4 parameters that important in this experiment. T_{cf} is cold finger temperature, T_{jac} is jacket temperature, t is time and rpm or speed of stir bar. However, there are just 2 parameters that varied in the experiment which are T_{cf} and time. Reservoir prepared by 5% by weight of wax is with mineral oil. First condition was performed at T_{jac} equals to 45 °C, T_{cf} equals to 5 °C, rpm equals to 240 and t equals to 30 min. Deposits were collected from cold finger and measure weight by scale. Figure 4.1 represents deposit that got from cold finger experiment at above condition.

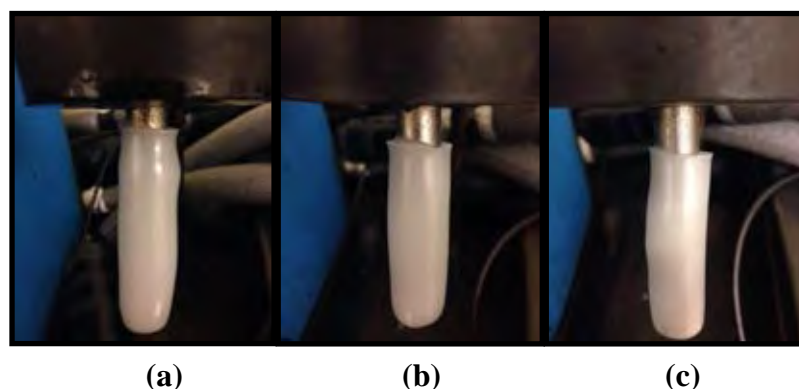


Figure 4.1 Deposit from cold finger experiment (a) uncoating (b) coating1 (c) coating2.

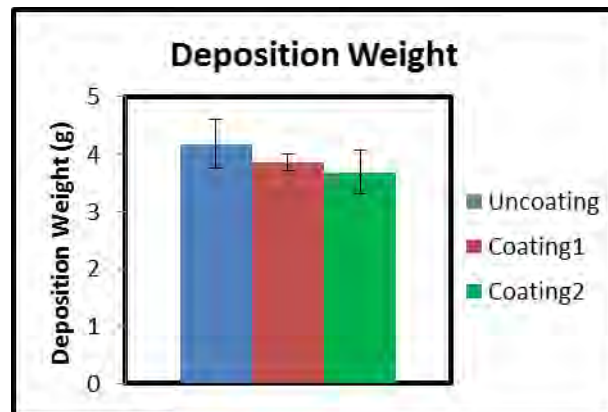


Figure 4.2 Deposit Weight from cold finger experiment in graph.

4.1.2 Wax Content

Figure 4.2 shows deposit weight from three cold fingers. It can be seen that weight of deposit from three cold fingers almost the same. It means that, there is no difference between uncoating, coating1 and coating2. After measure the weight from deposit, the next analysis is measured by HTGC in order to find the wax content.

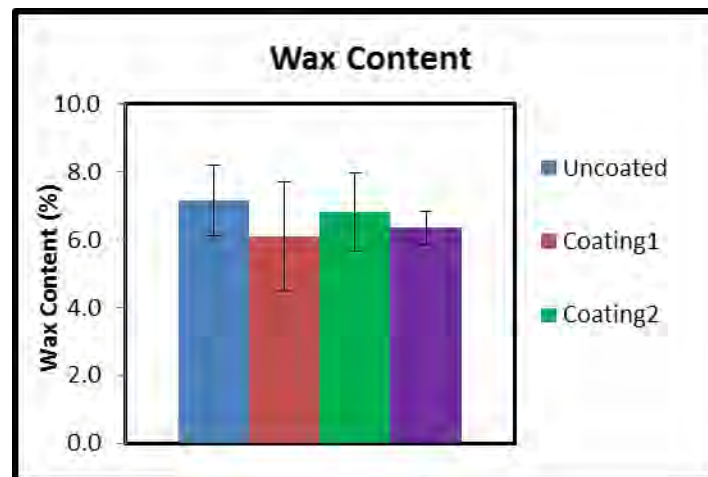


Figure 4.3 Wax content from cold finger experiment.

Figure 4.3 demonstrates the wax content from deposit on three cold fingers compare with model oil 5%Wax. It can be concluded that wax content of

deposit from uncoating cold finger is the same as deposit from coating1 and coating2 cold finger.

The trend of the results in deposit weight and wax content are the same from varies conditions. Those conditions are (i) T_{jac} equals to 45 °C, T_{cf} equals to 20°C, rpm equals to 240 and t equals to 30 min. (ii) T_{jac} equals to 45 °C, T_{cf} equals to 5°C, rpm equals to 240 and t equals to 1 min. (iii) T_{jac} equals to 45 °C, T_{cf} equals to 5°C, rpm equals to 240 and t equals to 3 min. (iv) T_{jac} equals to 45 °C, T_{cf} equals to 5°C, rpm equals to 240 and t equals to 5 min.

As the result, it turn out that the polymeric coating1 and coating2 are not work or reduce any deposition from cold finger experiment at above conditions. The hypothesis is that may be the shear force that provided from magnetic stir bar is sufficient to cause sloughing of deposit. From those reasons, then another topic of my research is investigated. It is about the kinetic study of wax deposition using cold finger apparatus.

4.2 Kinetic Study of Wax Deposition Using Cold Finger Apparatus

Second topic still keeps using the same apparatus which is cold finger apparatus. However, there is no comparison between polymeric anymore. It is focused on bare cold finger or the same as uncoated cold finger from previous topic. Important parameters also still keep the same which are T_{cf} is cold finger temperature, T_{jac} is jacket temperature, t is time and rpm or speed of stir bar. Three parameters are changed in order to see the effect on the deposit except T_{jac} . Reservoir is prepared by the same amount from first topic which is 5% of paraffin wax with mineral oil.

4.2.1 Effect of Rpm Changes

The condition is set at T_{jac} equals to 45 °C. T_{cf} equals to 5°C, t equals to 2 hr, rpm is changed from 0 rpm to 135 rpm and 240 rpm. Video was recording for the whole experiment in order to calculate the thickness. It can be seen that from Figure 4.4 that there is the thickness of deposit form immediately since cold finger dipped in the cold finger at all rpm. Then, it comes to the hypothesis that, it could be

another process during wax deposition apart from molecular diffusion which could be a process of gelation. The evolution of thickness is plot in Figure 4.4 but with different axis. Figure 4.4 a, y and z-axis are in normal scale. In 4.4 b, y axis is in normal scale and x axis is in log scale. In 6.4 c, both y and y-axis are log scale.

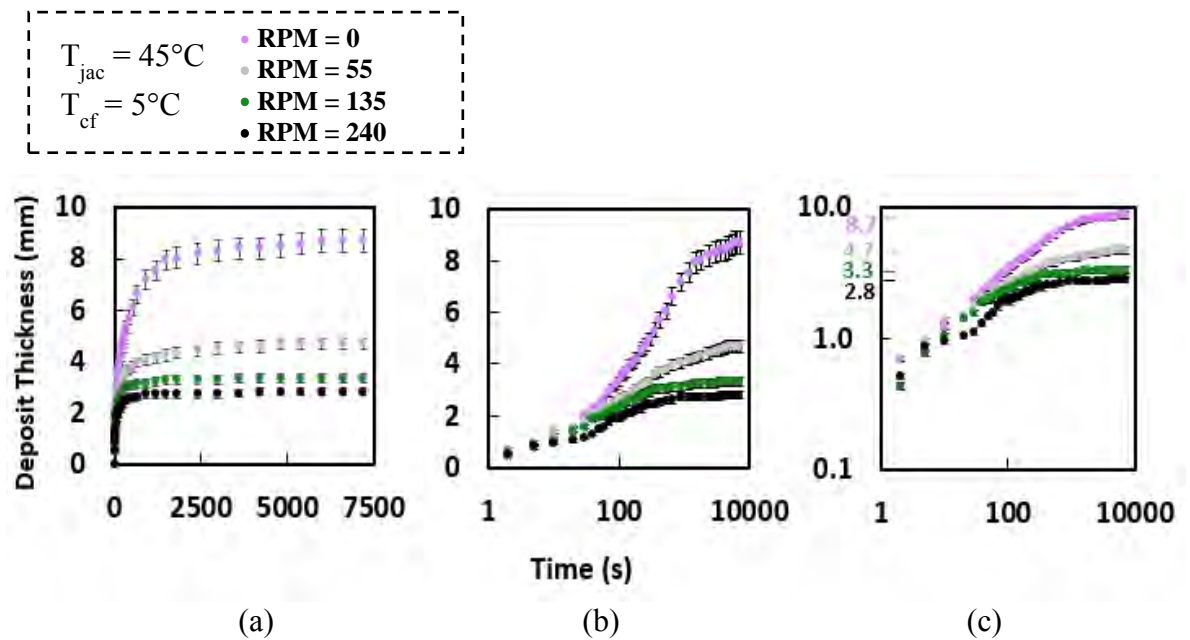


Figure 4.4 Thickness vs time when varies rpm.

4.2.2 Effect of Temperature Gradient on Deposit Formation

When Changing the Jacket Temperature

This experiment is set at T_{cf} equals to 5°C , rpm equals to 135 and t equals to 2hr, T_{jac} is changed from 5°C to 50°C and 52°C . From Figure 4.5, it can be concluded that as the temperature of jacket increases, the thickness of deposit is decreased as shown in Figure 4.5. Figure 4.5 a, y and z-axis are in normal scale. In 4.5 b, y axis is in normal scale and x axis is in log scale. In 4.5 c, both y and y-axis are log scale.

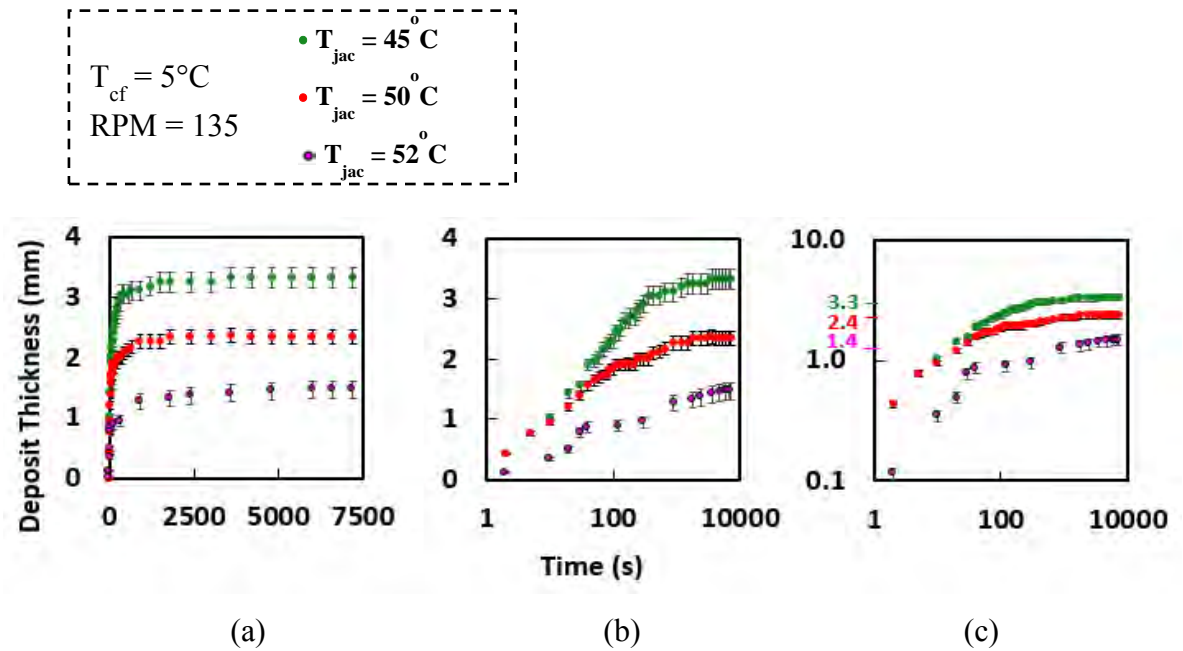


Figure 4.5 Thickness vs time when varies T_{jac} .

4.2.3 Effect of Temperature Gradient on Deposit Formation

When Changing the Cold Finger Temperature

This experiment is set at T_{jac} equals to 45°C , rpm equals to 135 and t equals to 2hr. T_{cf} is changed from 5°C , 15°C , 25°C and 35°C . From Figure 4.6, it can be concluded that as the temperature of cold finger increases, the thickness of deposit is decreased as shown in Figure 4.6. Figure 4.6 a, y and z-axis are in normal scale. In 4.6 b, y axis is in normal scale and x axis is in log scale. In 4.6 c, both y and y-axis are log scale.

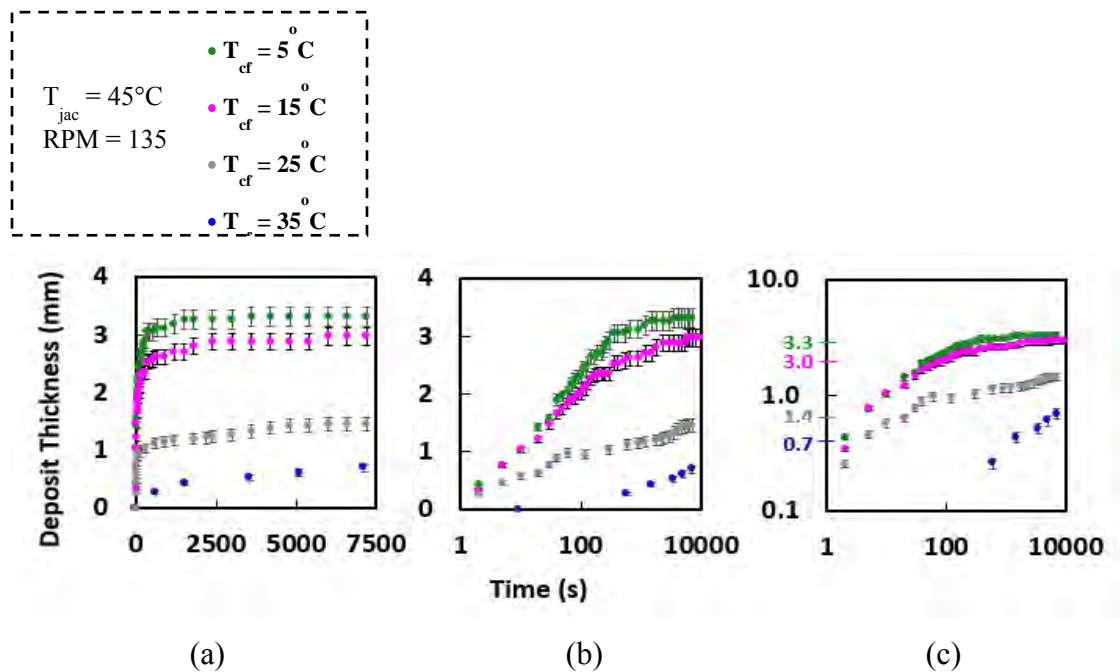


Figure 4.6 Deposit weight vs time at varies Tcf.

4.2.4 Final Thickness of Deposit : Deposit Thickness after 2 Hours of Experiment

Figure 4.7, shows the final thickness from all conditions that performed above. It can be concluded that final thickness decreases with increase of agitation rate, jacket temperature, and cold finger temperature. However, there is a question coming up when does the deposit stop growing?

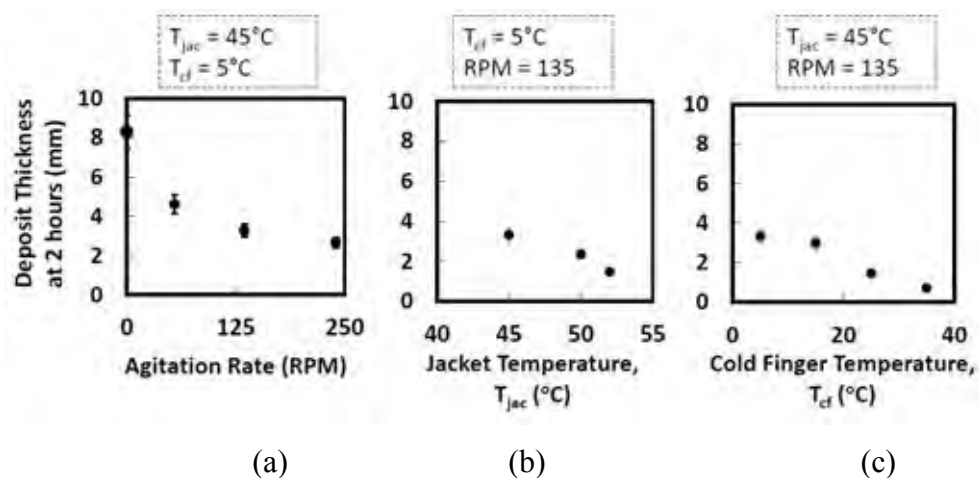


Figure 4.7 Final deposit thickness.

(a) varies RPM (b) varies different Tjac (c) varies Tcf

4.2.5 Temperature Profile of Fluid in Vessel at Steady State

In order to find the temperature across the cold finger apparatus, we need to use thermostat measure temperature at specific location through the cold finger apparatus at steady state of the condition: $T_{jac} = 45\text{ }^{\circ}\text{C}$, $\Delta T = 40\text{ }^{\circ}\text{C}$ and rpm = 240. It starts from inner diameter of jacket and another two positions farther from first location. The fourth and fifth location are chosen close to the wax deposit layer. The fifth point is at the surface of wax deposit. The last one is not from measurement but from the set point of chiller for the cold finger. As the result, temperature profile is started from cold finger temperature of $5\text{ }^{\circ}\text{C}$. Then, it increase to around $40\text{ }^{\circ}\text{C}$ at wax deposit surface before going up a bit $3\text{--}4\text{ }^{\circ}\text{C}$ and keep constant at bulk fluid. And, the inner jacket has a temperature of $44.5\text{ }^{\circ}\text{C}$. It represents in Figure 4.8.

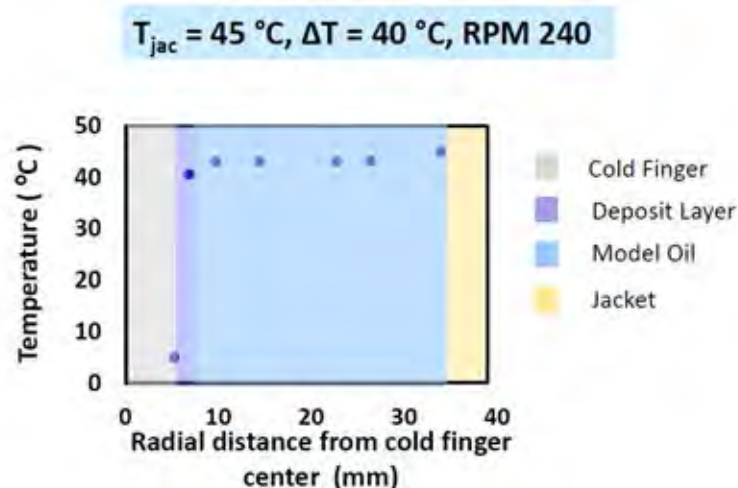


Figure 4.8 Temperature profile across cold finger.

4.2.6 Does Deposit Stops Growing Due to Wax Depletion in Oil?

Perform Mass Balance

There are two possibilities that why deposit stop growing. The first one, it could be because, wax depreciation and no deposit longer grows. The second hypothesis, wax stop growing because the interface temperature reach WAT. In order to test the first hypothesis, we take the sample of oil and wax mixture before run, after run and deposit. After that inject them to Gas Chromatography, GC. The

deposit is taken after it reach steady state which around two hours run. The experiment is set at $T_{jac} = 45\text{ }^{\circ}\text{C}$, $\Delta T = 40\text{ }^{\circ}\text{C}$ and $\text{rpm} = 135$. Figure 4.9, represents the procedure that described earlier. Figure 4.10, shows the GC result of oil before and oil after. It can be seen that oil after still remain waxes about the same as oil before. They also have the same WAT as well. As the result, it can be conclude that the wax deposit does not stop growing because of wax depreciation.

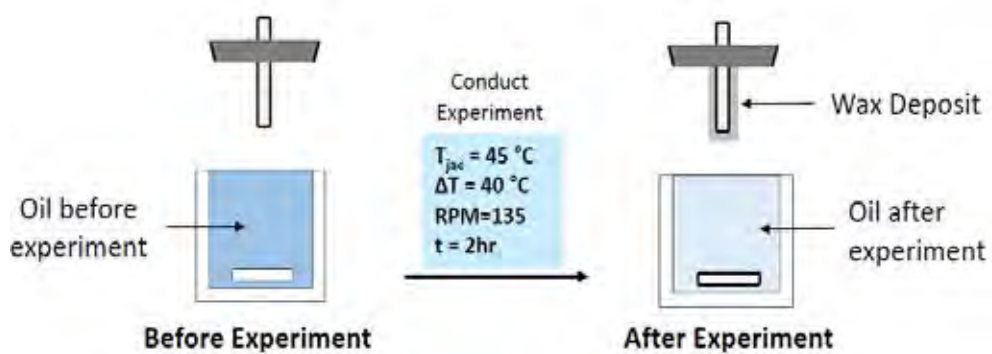


Figure 4.9 Find the mass balance in oil before, oil after and wax deposit.

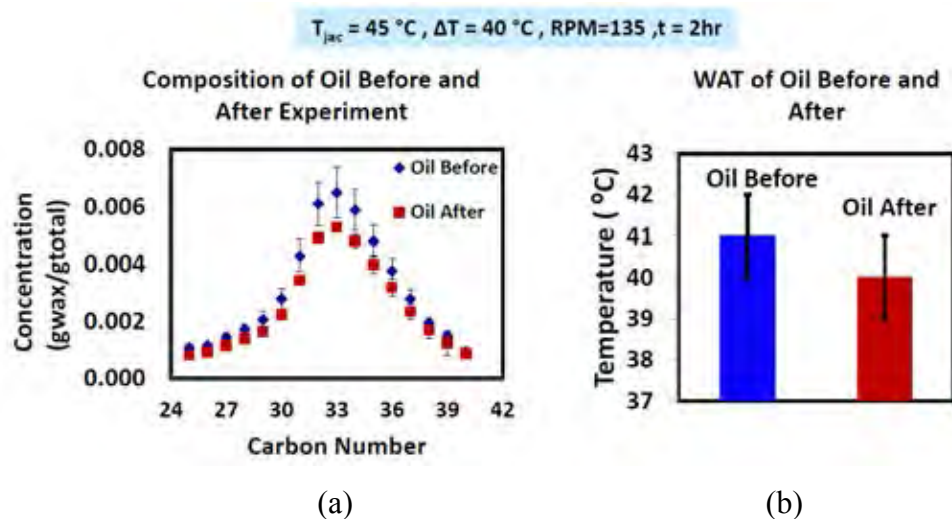


Figure 4.10 (a) Oil before and oil after wax composition (b) WAT of oil before and oil after.

4.2.7 Does Interface Reach Temperature equal to WAT of Oil ?

Calculation of Interface Temperature Based on Heat Flux

Temperature at deposit interface can be calculated based on the heat evolved through wax deposit at steady-state. Figure 4.11 represents the heat transfer diagram across cold finger apparatus. The interface temperature can be calculated using equation 29 through 31.

$$T_i = T_{cf} + q_{cf}\Omega_d \quad (29)$$

T_i is interface temperature, °C

T_{cf} is the cold finger temperature , °C

q_{cf} is heat transfer through cold finger, W/m²

Ω_d is heat transfer area, m²

$$q_{cf} = \dot{m}C_p(T_{out} - T_{in}) \quad (30)$$

\dot{m} is mass flow rate through cold finger, kg/sec

C_p is specific heat of water, J/kg.K

T_{out} is temperature of water out from cold finger, K

T_{in} is temperature of water into cold finger, K

$$\Omega_d = \frac{\ln(\frac{r_d}{R_c})}{2\pi kL} \quad (31)$$

r_d is thickness radius from center of cold finger, m

R_c is cold finger radius, m

k is thermal conductivity, W/m.K

L is cold finger length, m

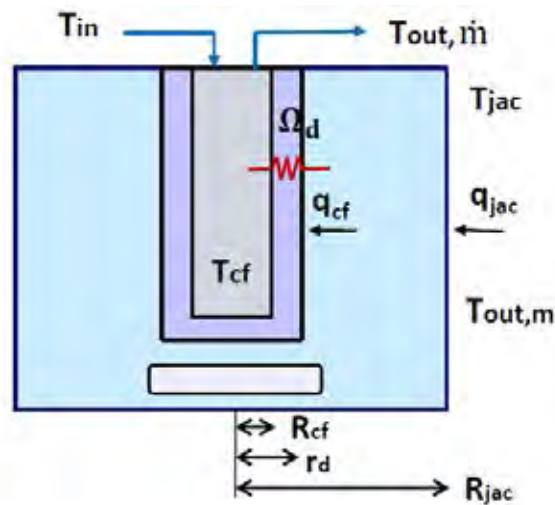


Figure 4.11 Heat transfer across sold finger apparatus.

First of all, we need to measure water flow rate through the cold finger. Water is from the chiller that set at a certain temperature. Jacket temperature also adjusted to a set point. Then measure temperature inlet and outlet from the cold finger. After the system reach steady state measure the thickness of wax deposit on the cold finger. Substitute all number in equation 29 to 31 to calculate T_i . Figure 4.12 shows T_i from 5 conditions in the table. It can be seen that the interface temperature, is the same WAT of 5%Wax in mineral which use in this experiment.

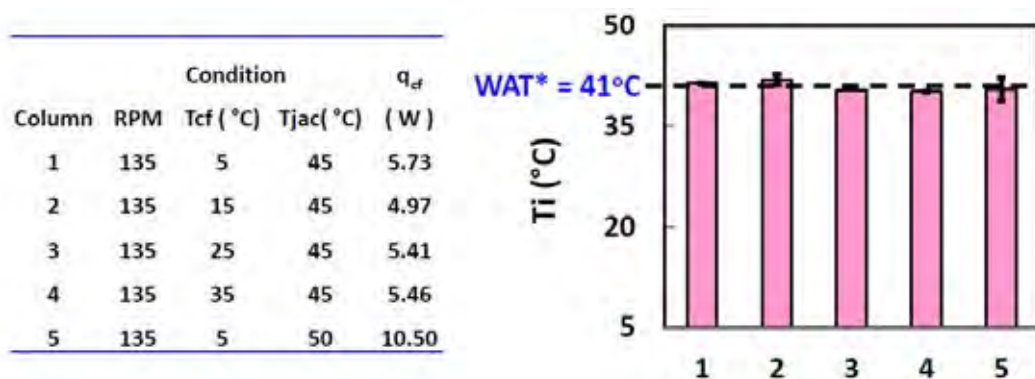


Figure 4.12 Interface temperature.

4.2.8 Final Deposit Thickness and Interface Temperature

Further Investigation on Final Deposit Thickness

Figure 4.13 represents the resistance through cold finger apparatus. There is three resistances in the jacket sides which from oil convection, glass conduction and water convection. In the cold finger side, there are two resistances which from deposit conduction and oil convection. We can use equation from 32 to 35 find the final deposit thickness. Firstly, heat transfer through jacket and cold finger are the same. Then, heat transfer through cold finger can be found by division of temperature differences from cold finger and the jacket with total resistances. Moreover, from equation 29, when we substitute all of known parameters, the final thickness can be calculated, r_d . The heat transfer coefficient is assumed to be 100 W/m.K .

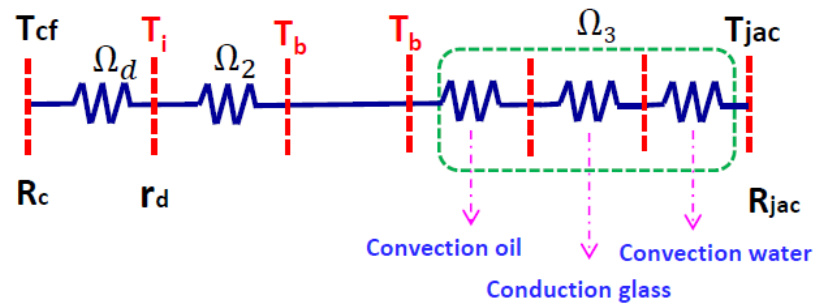


Figure 4.13 Resistances across cold finger.

At steady state, $q_{cf} = q_{jac}$

$$q_{cf} = \frac{\Delta T}{\Sigma \Omega} \quad (32)$$

$$T_i = T_{cf} + q_{cf} \Omega_d \quad (29)$$

$$T_i = T_{cf} + \left(\frac{T_{jac} - T_{cf}}{\frac{\ln(\frac{r_d}{R_c})}{2\pi k L} + \frac{1}{h_{cf} A_d} + \frac{1}{h_{jac} A_{jac}}} \right) \frac{\ln(\frac{r_d}{R_c})}{2\pi k L} \quad (33)$$

$$A_d = 2\pi r_d L + \pi r_d^2 \quad (34)$$

$$A_{jac} = 2\pi r_{jac} L + \pi r_{jac}^2 \quad (35)$$

4.2.9 Final Thickness and the Wax Appearance Temperature: Implication 1

After final deposit thickness can be calculated then we can explain that does the final thickness will be changed when WAT increases. From the heat transfer model or above equations that in section 4.2.8, the final deposit thickness will increase as WAT increases. It is due to how fast the system reaches WAT. Higher WAT, system needs more time to reach higher temperature as all of the conditions still remain the same which is shown in Figure 4.14.

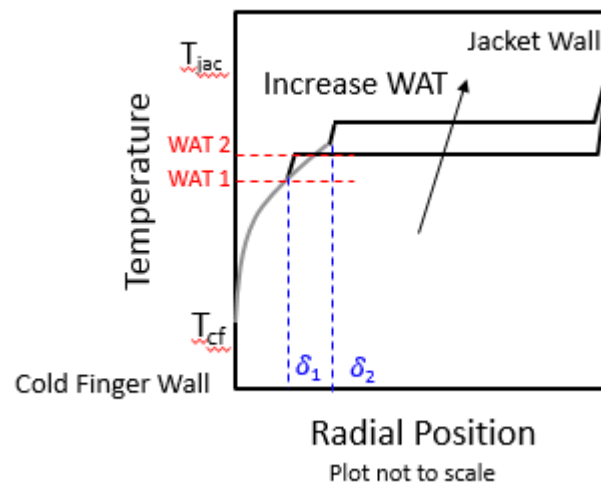
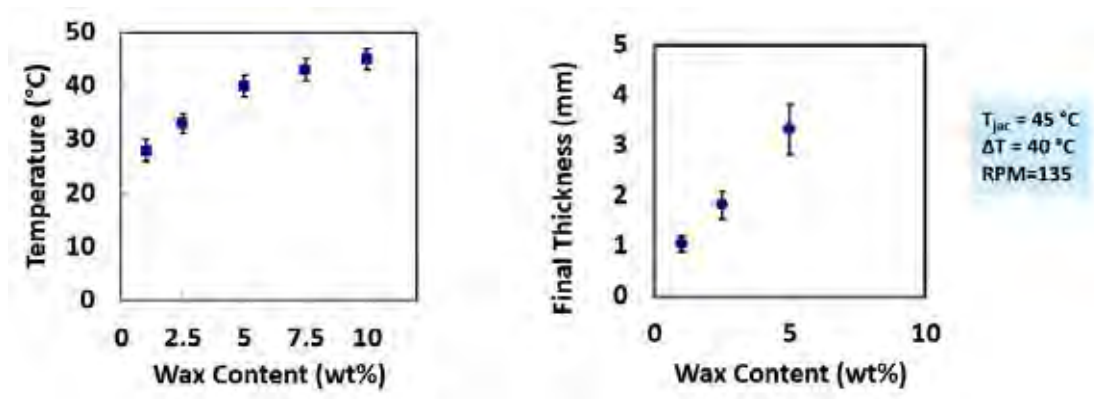


Figure 4.14 Temperature profile when WAT increases.

To confirm that the model is reliable, we perform laboratory experiment to support our model. The wax content is varied from 2.5 to 5, 7.5 and 10% weight. Because WAT will increase as wax content increases. The experiment is set at $T_{jac} = 45 \text{ }^\circ\text{C}$, $\Delta T = 40 \text{ }^\circ\text{C}$, $\text{rpm} = 135$ and deposition time is for 2 hr. After 2hr, the final thickness is measured and it is represented in Figure 4.15. As wax content increases or WAT increases, the final thickness increases as well. The experimental result is related to the model of heat transfer. So, the heat transfer model to find the final thickness is trustable.

Figure 4.15 Final wax deposit thickness when wax content increases.



4.2.10 Final Deposit Thickness and Interface Temperature : Implication 2

As the result, we can explain why final thickness of deposit reduces when rpm increases. It because of when rpm increases the system can reach WAT faster due to better heat transfer coefficient as represents in Figure 4.16.

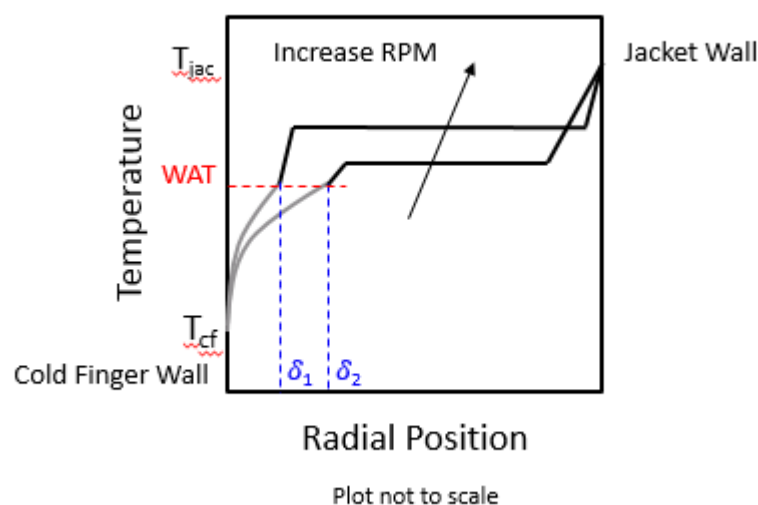


Figure 4.16 Final wax deposit thickness when rpm changes.

4.2.11 Evolution of Deposit Thickness When RPM changes

Final thickness is expected to decrease as RPM increases. Furthermore, the rpm is switched during the experiment, when first rpm already reach steady state. First experiment, starts deposition with agitation rate of 240rpm. After plateau on thickness, change agitation rate to 0 rpm. Second experiment, starts deposition with agitation rate of 0rpm. After plateau on thickness, change agitation

rate to 240 rpm. Both experiment set $T_{jac} = 45^{\circ}\text{C}$ and $\Delta T = 40^{\circ}\text{C}$. For first experiment, the deposit thickness increases when rpm is changed to be higher. In the second experiment the deposit thickness decreases when rpm is increased. The deposit thickness for both experiments are shown in Figure 4.17. The final wax deposit thickness will reach the same thickness as single rpm.

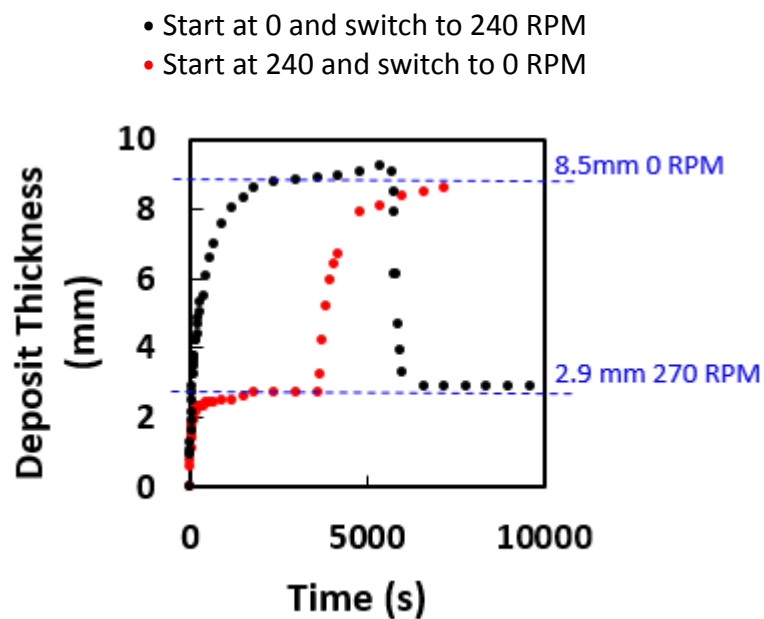


Figure 4.17 Wax deposit thickness when rpm changes.

4.2.12 Carbon Distribution

Figure 4.18 represents carbon distribution of the condition of the above condition. It can be compared that the composition of model oil 5%Wax is nearly identical to composition of deposit obtained with ΔT of 40°C in 1 min. The equality composition can be associated to gelation process. $\Delta T = 10^{\circ}\text{C}$ in 5 hr shift to the right as it contains more high carbon number. Different in deposit carbon composition is due to the mass transfer process.

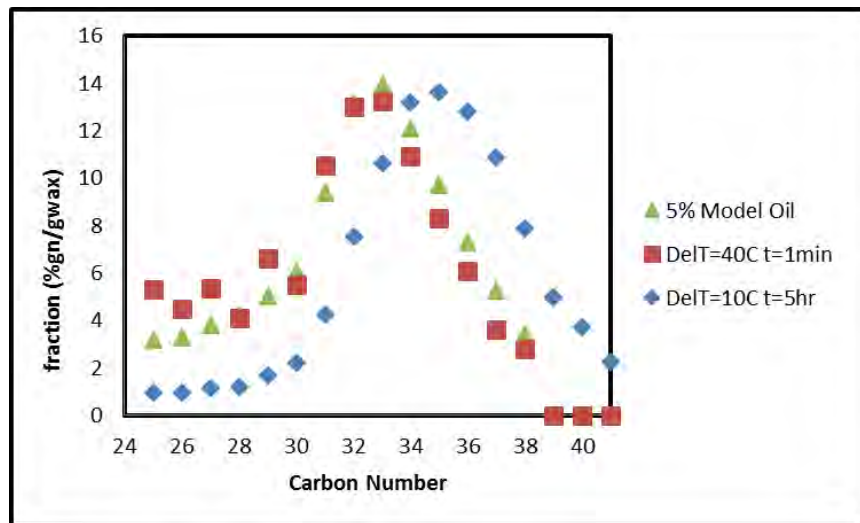


Figure 4.18 Carbon distribution.

4.2.13 Evolution of Thickness with Cooling Rate

This condition is performed at the base case of T_{jac} equals to 45 °C, rpm equals to 135, t equals to 3hr, T_{cf} at 5°C. However, T_{cf} is decreased manually by 1 °C from 45 °C to 5 °C. The cooling rate was around 0.38 °C/min. Figure 4.19 represents that thickness increased almost linearly. It can be explained temperature is the most important factor in gelation process which is a driving force of the wax mechanism.

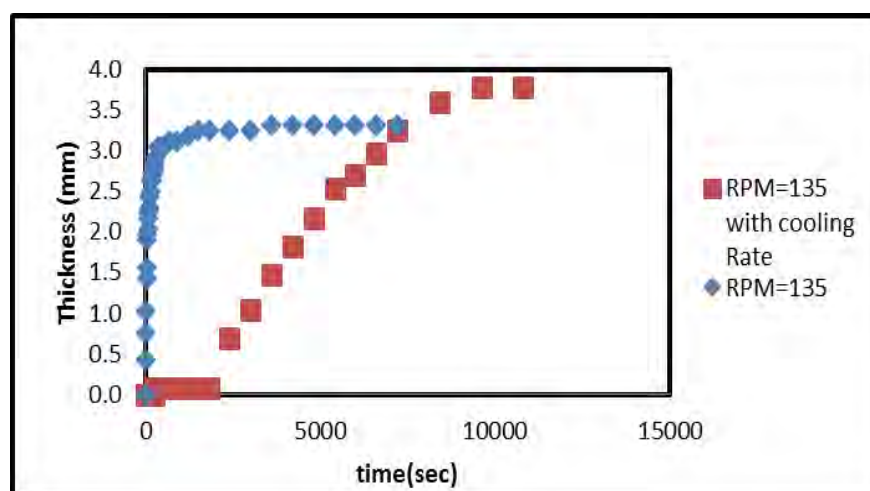


Figure 4.19 Thickness with cooling rate.

CHAPTER V

CONCLUSIONS AND RECOMMENDATIONS

From the first topic, it can be concluded that with uncoating cold finger, cold finger coated by polyurethane rubber and silicone (PDMS) rubber there are no differences in deposit mass and deposit wax content base on five conditions: i) T_{jac} equals to 45 °C, T_{cf} equals to 5°C, rpm equals to 135 and t equals to 2hr. ii) T_{jac} equals to 45 °C, T_{cf} equals to 20°C, rpm equals to 240 and t equals to 30 min. (iii) T_{jac} equals to 45 °C, T_{cf} equals to 5°C, rpm equals to 240 and t equals to 1 min. (iv) T_{jac} equals to 45 °C, T_{cf} equals to 5°C, rpm equals to 240 and t equals to 3 min. (v) T_{jac} equals to 45 °C, T_{cf} equals to 5°C, rpm equals to 240 and t equals to 5 min. As the result, they are not productive to improve for further application. The second topic

The second topic introduced another step in wax mechanism which is “gelation”. From the experiment gelation is a process that happens really fast. It occurs much faster than molecular diffusion. At lower rpm there is more wax deposit on cold finger. With a small ΔT condition, there fewer amounts of wax deposits on cold finger. So, the thickness of final deposit which can be measured from video recording at lower rpm will be thinner than higher rpm and thicker when ΔT is decreased. The wax carbon distribution of ΔT of 40 °C rpm=135 and t equals to 1 min has almost the same curve or distribution as 5% wax model oil. When ΔT reduced to 10 °C rpm=135 and t equals to 5 hr, the carbon curve shift to right as there is higher carbon deposit on cold surface. Gelation step is where there is exactly component of wax as the prepared reservoir or model oil. It indicates that temperature and time are important parameter for gelation. Moreover, when there is cooling rate apply to the system; the deposit thickness is in a linear line as the same as cooling rate. It also support that gelation is controlled by temperature gradient.

For moving forwards step, the model or fitting data will be applied to the lab results, in order to compare the theory and experiment. If it works out, then the gelation process will be more explainable in wax mechanisms.

APPENDICES

Appendix A Calibration Curve for Finding Thickness

The calibration curve has been constructed to find deposit thickness. We put ruler in the jacket which has a scale on then squeeze and expand the blue line and read the actual length from the ruler. Plot the measure length and actual length to get the calibration curve.

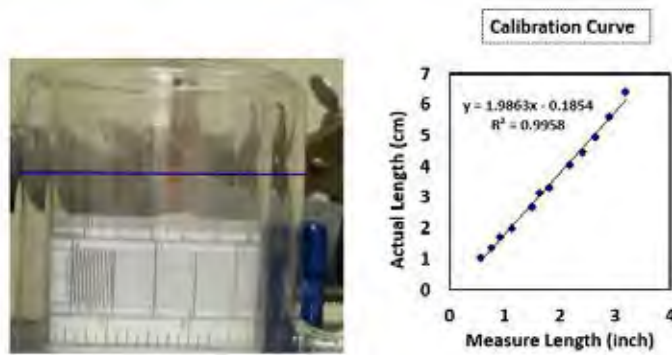


Figure A1 Calibration curve.

The technique was validated by comparing the actual mass of deposit with the mass calculated from thickness. The results show that they agree reasonably well to each another which means that the technique is applicable.

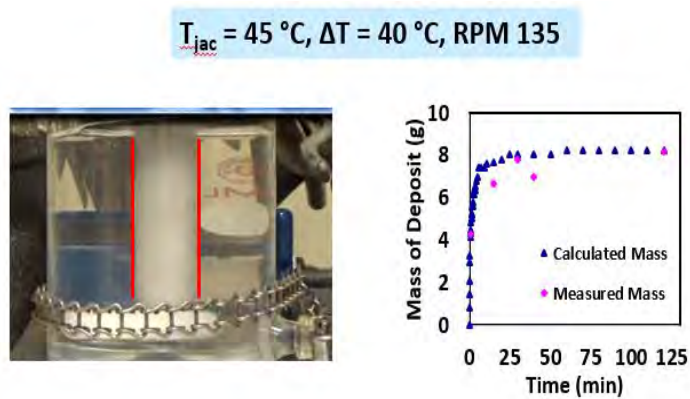


Figure A2 Comparison of calculated mass vs measured mass.

Table A1 Evolution of thickness at $T_{jac} = 45\text{ }^{\circ}\text{C}$, $\Delta T=40\text{ }^{\circ}\text{C}$, $\text{rpm}=0$, $t= 2\text{hr}$ at specific time

Measurement			Calculation	Error
time (sec)	time(min)	mass (g)	mass (g)	%
60	1	4.30	4.51	4.88
900	15	6.70	7.7	14.92
1800	30	7.80	8.05	3.20
2400	40	7.02	8.05	14.65
7200	120	8.18	8.27	1.11

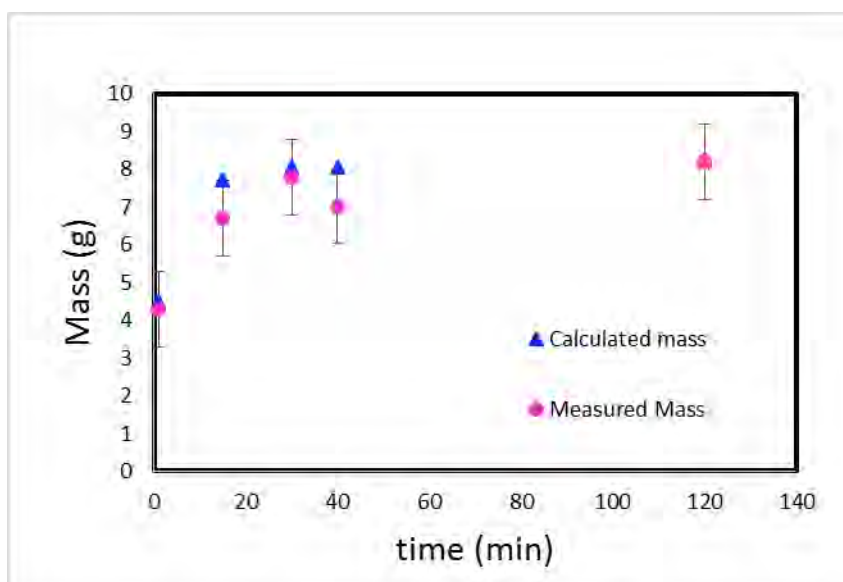


Figure A3 The error between calculated mass and measured mass.

The maximum %error is at time of 40 min which gives the error up to 14.6%. The remaining error is not more than 5%. They are not excellent agree to each another but it is in the acceptable range.

Appendix B Deposit Thickness When RPM Changes

Table B1 Evolution of thickness at $T_{jac} = 45\text{ }^{\circ}\text{C}$, $\Delta T = 40\text{ }^{\circ}\text{C}$, $\text{rpm} = 0$, $t = 2\text{ hr}$

t(sec)	diameter(mm)	Thickness(mm)	Volume(mm ³)	Volume(L)	mass(g)	Rate (mm/sec)	Mass Rate(g/sec)
0	10.5	0.00	0	0.000	0.000	0.000	0.000
2	12.2	0.86	1942	0.002	1.709	0.306	1.152
5	12.5	1.04	2374	0.002	2.089	0.122	0.468
10	12.7	1.12	2596	0.003	2.284	0.061	0.236
20	13.4	1.47	3520	0.004	3.098	0.031	0.121
30	14.5	2.00	5023	0.005	4.420	0.020	0.085
40	14.8	2.18	5555	0.006	4.889	0.015	0.064
50	15.2	2.35	6104	0.006	5.371	0.012	0.052
60	15.7	2.62	6958	0.007	6.123	0.010	0.044
70	15.9	2.71	7251	0.007	6.381	0.009	0.038
80	16.4	2.97	8100	0.008	7.128	0.008	0.034
90	16.6	3.06	8389	0.008	7.382	0.007	0.031
100	16.9	3.24	8978	0.009	7.901	0.016	0.074
110	17.1	3.33	9278	0.009	8.165	0.015	0.068
120	17.5	3.51	9889	0.010	8.702	0.014	0.063
130	17.8	3.69	10513	0.011	9.251	0.012	0.059
150	18.2	3.87	11151	0.011	9.813	0.011	0.052
170	18.6	4.05	11803	0.012	10.387	0.010	0.046
190	18.9	4.23	12470	0.012	10.973	0.009	0.042
220	19.3	4.41	13150	0.013	11.572	0.007	0.036
240	19.6	4.59	13846	0.014	12.184	0.007	0.034
260	20.2	4.86	14915	0.015	13.126	0.006	0.032
300	20.7	5.14	16018	0.016	14.096	0.005	0.028
360	21.7	5.60	17929	0.018	15.778	0.005	0.024
420	22.0	5.78	18720	0.019	16.474	0.004	0.021
540	23.1	6.33	21182	0.021	18.640	0.003	0.017
660	23.9	6.70	22899	0.023	20.151	0.002	0.014
900	25.0	7.26	25591	0.026	22.520	0.002	0.011
1200	26.1	7.83	28424	0.028	25.013	0.001	0.008
1500	26.9	8.20	30391	0.030	26.744	0.001	0.007
1800	27.1	8.30	30893	0.031	27.186	0.001	0.006
2400	27.3	8.39	31399	0.031	27.632	0.001	0.004
3000	27.6	8.58	32424	0.032	28.533	0.001	0.003
3600	27.8	8.68	32942	0.033	28.989	0.000	0.003
4200	28.0	8.77	33464	0.033	29.448	0.000	0.002
4800	28.0	8.77	33464	0.033	29.448	0.000	0.000
5400	28.2	8.87	33990	0.034	29.911	0.000	0.000
6000	28.2	8.87	33990	0.034	29.911	0.000	0.000
6600	28.2	8.87	33990	0.034	29.911	0.000	0.000
7200	28.2	8.87	33990	0.034	29.911		

Table B2 Evolution of thickness at $T_{jac} = 45\text{ }^{\circ}\text{C}$, $\Delta T = 40\text{ }^{\circ}\text{C}$, rpm=55, t= 2hr

t(sec)	diameter(mm)	Thickness(mm)	Volume(mm ³)	Volume(L)	mass(g)	Rate (mm/sec)	Mass Rate(g/sec)
0	10.5	0.00	0	0.000	0.000	0.000	0.000
2	11.7	0.60	1322	0.001	1.163	0.286	1.054
5	12.4	0.95	2157	0.002	1.898	0.114	0.435
10	13.2	1.39	3283	0.003	2.889	0.057	0.226
20	13.4	1.47	3520	0.004	3.098	0.029	0.114
30	13.9	1.74	4254	0.004	3.743	0.019	0.077
40	14.6	2.09	5287	0.005	4.652	0.014	0.060
50	14.6	2.09	5287	0.005	4.652	0.011	0.048
60	15.0	2.26	5827	0.006	5.128	0.010	0.040
70	15.2	2.35	6104	0.006	5.371	0.008	0.035
80	15.3	2.44	6434	0.006	5.662	0.007	0.031
90	15.5	2.53	6703	0.007	5.899	0.006	0.027
100	15.7	2.62	6976	0.007	6.139	0.006	0.025
110	15.9	2.71	7252	0.007	6.381	0.005	0.023
120	15.9	2.71	7252	0.007	6.381	0.005	0.021
130	16.1	2.80	7531	0.008	6.627	0.004	0.019
150	16.1	2.80	7531	0.008	6.627	0.004	0.017
170	16.2	2.88	7814	0.008	6.876	0.003	0.015
190	16.6	3.06	8389	0.008	7.382	0.003	0.014
220	16.8	3.15	8682	0.009	7.640	0.003	0.012
240	16.8	3.15	8682	0.009	7.640	0.002	0.011
260	16.9	3.24	8978	0.009	7.901	0.002	0.010
300	17.1	3.33	9278	0.009	8.165	0.002	0.009
360	17.7	3.60	10199	0.010	8.975	0.002	0.007
420	17.8	3.69	10513	0.011	9.251	0.001	0.006
540	18.2	3.87	11151	0.011	9.813	0.001	0.005
660	18.4	3.96	11475	0.011	10.098	0.001	0.004
900	18.6	4.05	11803	0.012	10.387	0.001	0.003
1200	18.7	4.14	12135	0.012	10.678	0.000	0.002
1500	18.9	4.23	12470	0.012	10.973	0.000	0.002
1800	19.1	4.32	12808	0.013	11.271	0.000	0.002
2400	19.3	4.41	13150	0.013	11.572	0.000	0.001
3000	19.5	4.50	13496	0.013	11.877	0.000	0.001
3600	19.6	4.59	13846	0.014	12.184	0.000	0.001
4200	19.6	4.59	13846	0.014	12.184	0.000	0.001
4800	19.8	4.68	14199	0.014	12.495	0.000	0.001
5400	19.8	4.68	14199	0.014	12.495	0.000	0.000
6000	19.8	4.68	14199	0.014	12.495	0.000	0.000
6600	19.8	4.68	14199	0.014	12.495	0.000	0.000
7200	19.8	4.68	14199	0.014	12.495		

Table B3 Evolution of thickness at $T_{jac} = 45\text{ }^{\circ}\text{C}$, $\Delta T = 40\text{ }^{\circ}\text{C}$, rpm=135, t= 2hr

t(sec)	diameter(mm)	Thickness(mm)	Volume(mm ³)	Volume(L)	mass(g)	Rate (mm/sec)	Mass Rate(g/sec)
0	10.46	0.00	0.000	0.000	0.000	0.000	0.000
2	11.32	0.43	926.575	0.001	0.815	0.262	0.950
5	11.99	0.76	1695.965	0.002	1.492	0.105	0.391
10	12.52	1.03	2350.013	0.002	2.068	0.052	0.200
20	13.32	1.43	3396.907	0.003	2.989	0.026	0.104
30	13.59	1.56	3763.768	0.004	3.312	0.017	0.070
40	14.26	1.90	4720.901	0.005	4.154	0.013	0.054
50	14.39	1.96	4919.269	0.005	4.329	0.010	0.043
60	14.53	2.03	5119.977	0.005	4.506	0.009	0.036
70	14.80	2.17	5528.457	0.006	4.865	0.007	0.031
80	14.93	2.23	5736.251	0.006	5.048	0.007	0.028
90	15.07	2.30	5946.430	0.006	5.233	0.006	0.025
100	15.07	2.30	5946.430	0.006	5.233	0.005	0.022
110	15.34	2.44	6373.987	0.006	5.609	0.005	0.020
120	15.34	2.44	6373.987	0.006	5.609	0.004	0.019
130	15.47	2.51	6591.388	0.007	5.800	0.004	0.017
150	15.75	2.64	7033.492	0.007	6.189	0.003	0.015
170	15.75	2.64	7033.492	0.007	6.189	0.003	0.013
190	15.88	2.71	7258.217	0.007	6.387	0.003	0.012
220	15.88	2.71	7258.217	0.007	6.387	0.002	0.010
240	16.02	2.78	7485.407	0.007	6.587	0.002	0.010
260	16.15	2.84	7715.073	0.008	6.789	0.002	0.009
300	16.29	2.91	7947.226	0.008	6.994	0.002	0.008
360	16.56	3.05	8419.042	0.008	7.409	0.001	0.007
420	16.56	3.05	8419.042	0.008	7.409	0.001	0.006
540	16.56	3.05	8419.042	0.008	7.409	0.000	0.001
660	16.70	3.12	8658.728	0.009	7.620	0.000	0.001
900	16.75	3.14	8749.791	0.009	7.700	0.000	0.001
1200	16.84	3.19	8900.948	0.009	7.833	0.000	0.001
1500	16.97	3.25	9145.713	0.009	8.048	0.000	0.001
1800	16.97	3.25	9145.713	0.009	8.048	0.000	0.000
2400	16.97	3.25	9145.713	0.009	8.048	0.000	0.000
3000	16.97	3.25	9145.713	0.009	8.048	0.000	0.000
3600	17.11	3.32	9393.037	0.009	8.266	0.000	0.000
4200	17.11	3.32	9393.037	0.009	8.266	0.000	0.000
4800	17.11	3.32	9393.037	0.009	8.266	0.000	0.000
5400	17.11	3.32	9393.037	0.009	8.266	0.000	0.000
6000	17.11	3.32	9393.037	0.009	8.266	0.000	0.000
6600	17.11	3.32	9393.037	0.009	8.266	0.000	0.000
7200	17.11	3.32	9393.037	0.009	8.266		

Table B4 Evolution of thickness at $T_{jac} = 45\text{ }^{\circ}\text{C}$, $\Delta T = 40\text{ }^{\circ}\text{C}$, rpm=240, t= 2hr

t(sec)	diameter(mm)	Thickness(mm)	Volume(mm ³)	Volume(L)	mass(g)	Rate (mm/sec)	Mass Rate(g/sec)
0	10.5	0.00	343.797	0.000	0.303	0.000	0.000
2	11.8	0.69	1844.824	0.002	1.623	0.191	0.709
5	12.2	0.86	2255.518	0.002	1.985	0.076	0.288
10	12.4	0.95	2466.308	0.002	2.170	0.038	0.145
20	12.5	1.04	2680.758	0.003	2.359	0.019	0.073
30	12.7	1.12	2898.892	0.003	2.551	0.013	0.049
40	13.1	1.30	3346.308	0.003	2.945	0.010	0.037
50	13.4	1.47	3808.746	0.004	3.352	0.008	0.030
60	13.6	1.56	4045.658	0.004	3.560	0.006	0.025
70	13.9	1.74	4530.991	0.005	3.987	0.005	0.022
80	14.3	1.91	5031.830	0.005	4.428	0.005	0.020
90	14.3	1.91	5031.830	0.005	4.428	0.004	0.017
100	14.3	1.91	5031.830	0.005	4.428	0.004	0.016
110	14.3	1.91	5031.830	0.005	4.428	0.003	0.014
120	14.5	2.00	5288.126	0.005	4.654	0.003	0.013
130	14.6	2.09	5548.372	0.006	4.883	0.003	0.012
150	14.6	2.09	5548.372	0.006	4.883	0.003	0.011
170	14.8	2.18	5812.594	0.006	5.115	0.002	0.009
190	15.0	2.26	6080.815	0.006	5.351	0.002	0.009
220	15.0	2.26	6080.815	0.006	5.351	0.002	0.007
240	15.2	2.35	6353.062	0.006	5.591	0.002	0.007
300	15.3	2.44	6629.359	0.007	5.834	0.001	0.005
360	15.3	2.44	6629.359	0.007	5.834	0.001	0.005
420	15.3	2.44	6629.359	0.007	5.834	0.001	0.004
540	15.5	2.53	6909.731	0.007	6.081	0.001	0.003
660	15.5	2.53	6909.731	0.007	6.081	0.001	0.003
780	15.7	2.62	7194.204	0.007	6.331	0.000	0.002
900	15.9	2.71	7482.803	0.007	6.585	0.000	0.002
1200	15.9	2.71	7482.803	0.007	6.585	0.000	0.000
1500	15.9	2.71	7482.803	0.007	6.585	0.000	0.000
1800	15.9	2.71	7482.803	0.007	6.585	0.000	0.000
2400	15.9	2.71	7482.803	0.007	6.585	0.000	0.000
3000	15.9	2.71	7482.803	0.007	6.585	0.000	0.000
3600	16.1	2.80	7758.300	0.008	6.827	0.000	0.000
4200	16.1	2.80	7758.300	0.008	6.827	0.000	0.000
4800	16.1	2.80	7758.300	0.008	6.827	0.000	0.000
5400	16.1	2.80	7758.300	0.008	6.827	0.000	0.000
6000	16.1	2.80	7758.300	0.008	6.827	0.000	0.000
6600	16.1	2.80	7758.300	0.008	6.827	0.000	0.000
7200	16.1	2.80	7758.305	0.008	6.827		

Appendix C Deposit Thickness When Jacket Temperature Changes

Table C1 Evolution of thickness at $T_{jac} = 50\text{ }^{\circ}\text{C}$, $\Delta T = 45\text{ }^{\circ}\text{C}$, rpm=135, $t = 2\text{ hr}$

t(sec)	diameter(mm)	Thickness(mm)	Volume(mm ³)	Volume(L)	mass(g)	Rate (mm/sec)	Mass Rate(g/sec)
0	10.46	0.00	0.000	0.000	0.000	0.000	0.000
2	11.32	0.43	926.575	0.001	0.815	0.311	0.272
5	12.02	0.78	1731.967	0.002	1.524	0.130	0.305
10	12.36	0.95	2156.554	0.002	1.898	0.058	0.190
20	12.89	1.21	2821.329	0.003	2.483	0.044	0.248
30	13.23	1.39	3283.388	0.003	2.889	0.035	0.289
40	13.58	1.56	3760.774	0.004	3.309	0.026	0.331
50	13.76	1.65	4005.274	0.004	3.525	0.009	0.352
60	13.76	1.65	4005.274	0.004	3.525	0.009	0.352
70	13.93	1.74	4253.679	0.004	3.743	0.009	0.374
80	13.93	1.74	4253.679	0.004	3.743	0.009	0.374
90	14.11	1.82	4506.013	0.005	3.965	0.009	0.397
100	14.11	1.82	4506.013	0.005	3.965	0.009	0.397
110	14.29	1.91	4762.301	0.005	4.191	0.009	0.419
120	14.29	1.91	4762.301	0.005	4.191	0.000	0.419
130	14.29	1.91	4762.301	0.005	4.191	0.000	0.210
150	14.29	1.91	4762.301	0.005	4.191	0.000	0.210
170	14.29	1.91	4762.301	0.005	4.191	0.000	0.210
190	14.29	1.91	4762.301	0.005	4.191	0.000	0.140
220	14.29	1.91	4762.301	0.005	4.191	0.004	0.210
240	14.46	2.00	5022.567	0.005	4.420	0.004	0.221
260	14.46	2.00	5022.567	0.005	4.420	0.000	0.110
300	14.46	2.00	5022.567	0.005	4.420	0.000	0.074
360	14.46	2.00	5022.567	0.005	4.420	0.001	0.074
420	14.64	2.09	5286.837	0.005	4.652	0.001	0.039
540	14.64	2.09	5286.837	0.005	4.652	0.001	0.039
660	14.81	2.18	5555.135	0.006	4.889	0.001	0.020
900	14.99	2.26	5827.487	0.006	5.128	0.000	0.017
1200	14.99	2.26	5827.487	0.006	5.128	0.000	0.017
1500	14.99	2.26	5827.487	0.006	5.128	0.000	0.017
1800	15.17	2.35	6103.917	0.006	5.371	0.000	0.009
2400	15.17	2.35	6103.917	0.006	5.371	0.000	0.009
3000	15.17	2.35	6103.917	0.006	5.371	0.000	0.009
3600	15.17	2.35	6103.917	0.006	5.371	0.000	0.009
4200	15.17	2.35	6103.917	0.006	5.371	0.000	0.009
4800	15.17	2.35	6103.917	0.006	5.371	0.000	0.009
5400	15.17	2.35	6103.917	0.006	5.371	0.000	0.009
6000	15.17	2.35	6103.917	0.006	5.371	0.000	0.009
6600	15.17	2.35	6103.917	0.006	5.371	0.000	0.009
7200	15.17	2.35	6103.917	0.006	5.371		

Table C2 Evolution of thickness at $T_{jac} = 52\text{ }^{\circ}\text{C}$, $\Delta T = 47\text{ }^{\circ}\text{C}$, $\text{rpm} = 135$, $t = 2\text{ hr}$

t(sec)	diameter(mm)	Thickness(mm)	Volume(mm ³)	Volume(L)	mass(g)	Rate (mm/sec)	Mass Rate(g/sec)
0	10.46	0.00	0.000	0.000	0.000	0.000	0.000
2	10.69	0.11	238.678	0.000	0.210	0.069	0.026
10	11.15	0.34	734.842	0.001	0.647	0.042	0.065
20	11.44	0.49	1057.473	0.001	0.931	0.043	0.093
30	12.02	0.78	1732.043	0.002	1.524	0.037	0.152
40	12.19	0.86	1942.494	0.002	1.709	0.003	0.021
120	12.25	0.89	2013.489	0.002	1.772	0.001	0.010
300	12.36	0.95	2157.263	0.002	1.898	0.001	0.003
900	13.00	1.27	2973.853	0.003	2.617	0.001	0.003
1800	13.12	1.33	3127.788	0.003	2.752	0.000	0.005
2400	13.20	1.37	3236.884	0.003	2.848	0.000	0.002
3600	13.29	1.41	3361.912	0.003	2.958	0.000	0.002
4800	13.35	1.44	3439.229	0.003	3.027	0.000	0.003
6000	13.41	1.47	3520.240	0.004	3.098	0.000	0.005
6600	13.41	1.47	3520.240	0.004	3.098	0.000	0.005
7200	13.41	1.47	3520.240	0.004	3.098	0.002	0.000

Appendix D Deposit Thickness When Cold Finger Temperature Changes

Table D1 Evolution of thickness at $T_{jac} = 45\text{ }^{\circ}\text{C}$, $\Delta T = 10\text{ }^{\circ}\text{C}$, rpm=135, t= 3hr

t(sec)	diameter(mm)	Thickness(mm)	Volume(mm ³)	Volume(L)	mass(g)	Rate (mm/sec)	Mass Rate(g/sec)
0	10.12	0.00	0.000	0.000	0.000	0.000	0.000
2	10.46	0.17	347.231	0.000	0.306	0.103	0.102
5	10.64	0.26	526.031	0.001	0.463	0.021	0.093
10	10.64	0.26	526.031	0.001	0.463	0.000	0.046
20	10.64	0.26	526.031	0.001	0.463	0.000	0.046
30	10.64	0.26	526.031	0.001	0.463	0.000	0.046
40	10.64	0.26	526.031	0.001	0.463	0.000	0.046
50	10.64	0.26	526.031	0.001	0.463	0.000	0.046
60	10.64	0.26	526.031	0.001	0.463	0.000	0.046
70	10.64	0.26	526.031	0.001	0.463	0.000	0.046
80	10.64	0.26	526.031	0.001	0.463	0.000	0.046
90	10.64	0.26	526.031	0.001	0.463	0.009	0.046
100	10.81	0.34	708.318	0.001	0.623	0.009	0.062
110	10.81	0.34	708.318	0.001	0.623	0.000	0.062
120	10.81	0.34	708.318	0.001	0.623	0.000	0.062
130	10.81	0.34	708.318	0.001	0.623	0.000	0.031
150	10.81	0.34	708.318	0.001	0.623	0.000	0.031
170	10.81	0.34	708.318	0.001	0.623	0.000	0.031
190	10.81	0.34	708.318	0.001	0.623	0.000	0.021
220	10.81	0.34	708.318	0.001	0.623	0.000	0.031
240	10.81	0.34	708.318	0.001	0.623	0.004	0.031
260	10.98	0.43	894.115	0.001	0.787	0.003	0.020
300	10.98	0.43	894.115	0.001	0.787	0.000	0.013
360	10.98	0.43	894.115	0.001	0.787	0.000	0.013
420	10.98	0.43	894.115	0.001	0.787	0.000	0.007
540	10.98	0.43	894.115	0.001	0.787	0.001	0.007
660	11.15	0.52	1083.444	0.001	0.953	0.000	0.004
900	11.15	0.52	1083.444	0.001	0.953	0.000	0.003
1200	11.15	0.52	1083.444	0.001	0.953	0.000	0.003
1500	11.32	0.60	1276.330	0.001	1.123	0.000	0.004
1800	11.32	0.60	1276.330	0.001	1.123	0.000	0.002
2400	11.32	0.60	1276.330	0.001	1.123	0.000	0.002
3000	11.50	0.69	1472.794	0.001	1.296	0.000	0.002
3600	11.50	0.69	1472.794	0.001	1.296	0.000	0.002
4200	11.50	0.69	1472.794	0.001	1.296	0.000	0.002
4800	11.67	0.77	1672.861	0.002	1.472	0.000	0.002
5400	11.67	0.77	1672.861	0.002	1.472	0.000	0.002
6000	11.84	0.86	1876.554	0.002	1.651	0.000	0.003
6600	11.84	0.86	1876.554	0.002	1.651	0.000	0.003
7200	11.84	0.86	1876.554	0.002	1.651	0.000	0.001
8400	11.84	0.86	1876.554	0.002	1.651	0.000	0.001
9600	11.84	0.86	1876.554	0.002	1.651	0.000	0.001
10800	11.84	0.86	1876.554	0.002	1.651		

Table D2 Evolution of thickness at $T_{jac} = 45\text{ }^{\circ}\text{C}$, $\Delta T = 20\text{ }^{\circ}\text{C}$, rpm=135, t= 2hr

t(sec)	diameter(mm)	Thickness(mm)	Volume(mm ³)	Volume(L)	mass(g)	Rate (mm/sec)	Mass Rate(g/sec)
0	10.46	0.00	0.000	0.000	0.000	0.000	0.000
2	10.98	0.26	545.670	0.001	0.480	0.184	0.160
5	11.38	0.46	991.656	0.001	0.873	0.079	0.175
10	11.61	0.57	1255.298	0.001	1.105	0.023	0.110
20	11.73	0.63	1389.448	0.001	1.223	0.020	0.122
30	12.02	0.78	1731.967	0.002	1.524	0.026	0.152
40	12.25	0.89	2013.567	0.002	1.772	0.012	0.089
60	12.36	0.95	2156.633	0.002	1.898	0.002	0.032
120	12.42	0.98	2226.968	0.002	1.960	0.001	0.011
300	12.54	1.04	2374.482	0.002	2.090	0.001	0.007
600	12.71	1.12	2596.068	0.003	2.285	0.000	0.008
900	12.77	1.15	2670.872	0.003	2.350	0.000	0.008
1200	12.80	1.17	2710.151	0.003	2.385	0.000	0.004
1800	12.85	1.19	2774.974	0.003	2.442	0.000	0.006
2200	12.90	1.22	2840.087	0.003	2.499	0.000	0.012
2400	12.95	1.24	2905.490	0.003	2.557	0.000	0.004
3000	13.00	1.27	2971.185	0.003	2.615	0.000	0.004
3600	13.12	1.33	3128.463	0.003	2.753	0.000	0.005
4200	13.24	1.39	3283.985	0.003	2.890	0.000	0.005
4800	13.30	1.42	3371.488	0.003	2.967	0.000	0.005
5400	13.32	1.43	3398.549	0.003	2.991	0.000	0.005
6000	13.35	1.44	3441.350	0.003	3.028	0.000	0.005
6600	13.35	1.44	3441.350	0.003	3.028	0.000	0.005
7200	13.35	1.44	3440.801	0.003	3.028		

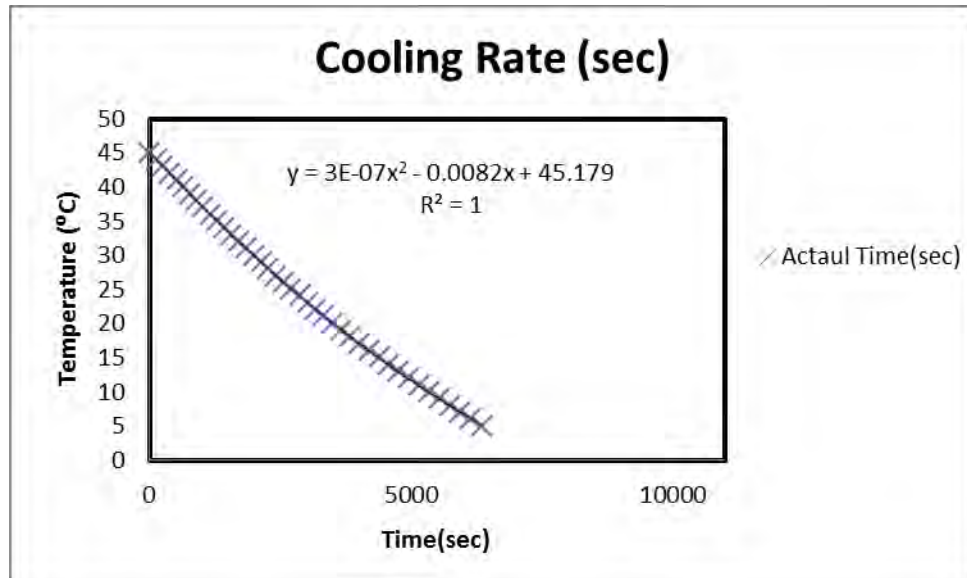
Appendix E Thickness With Cooling Rate**Figure E1** Cooling rate.

Table E1 Evolution of thickness at $T_{jac} = 45\text{ }^{\circ}\text{C}$, $\Delta T=40\text{ }^{\circ}\text{C}$, rpm=135, t= 3hr with cooling rate

t(sec)	diameter(mm)	Thickness(mm)	Volume(mm ³)	Volume(L)	mass(g)	Rate (mm/sec)	Mass Rate(g/sec)
0	10.46	0.00	0.000	0.000	0.000	0.000	0.000
2	10.46	0.00	0.000	0.000	0.000	0.000	0.000
5	10.46	0.00	0.000	0.000	0.000	0.000	0.000
10	10.46	0.00	0.000	0.000	0.000	0.000	0.000
20	10.46	0.00	0.000	0.000	0.000	0.000	0.000
30	10.46	0.00	0.000	0.000	0.000	0.000	0.000
40	10.46	0.00	0.000	0.000	0.000	0.000	0.000
50	10.46	0.00	0.000	0.000	0.000	0.000	0.000
60	10.46	0.00	0.000	0.000	0.000	0.000	0.000
70	10.46	0.00	0.000	0.000	0.000	0.000	0.000
80	10.46	0.00	0.000	0.000	0.000	0.000	0.000
90	10.46	0.00	0.000	0.000	0.000	0.000	0.000
100	10.46	0.00	0.000	0.000	0.000	0.000	0.000
110	10.46	0.00	0.000	0.000	0.000	0.000	0.000
120	10.46	0.00	0.000	0.000	0.000	0.000	0.000
130	10.46	0.00	0.000	0.000	0.000	0.000	0.000
150	10.46	0.00	0.000	0.000	0.000	0.000	0.000
170	10.46	0.00	0.000	0.000	0.000	0.000	0.000
190	10.46	0.00	0.000	0.000	0.000	0.000	0.000
220	10.46	0.00	0.000	0.000	0.000	0.000	0.000
240	10.46	0.00	0.000	0.000	0.000	0.004	0.000
260	10.64	0.09	178.312	0.000	0.157	0.003	0.004
300	10.64	0.09	178.312	0.000	0.157	0.000	0.003
360	10.64	0.09	178.312	0.000	0.157	0.000	0.003
420	10.64	0.09	178.312	0.000	0.157	0.000	0.001
540	10.64	0.09	178.312	0.000	0.157	0.000	0.001
660	10.64	0.09	178.312	0.000	0.157	0.000	0.001
900	10.64	0.09	178.312	0.000	0.157	0.000	0.001
1200	10.64	0.09	178.312	0.000	0.157	0.000	0.001
1500	10.64	0.09	178.312	0.000	0.157	0.000	0.001
1800	10.64	0.09	178.312	0.000	0.157	0.001	0.000
2400	11.84	0.69	1525.182	0.002	1.342	0.002	0.002
3000	12.54	1.04	2374.402	0.002	2.089	0.001	0.003
3600	13.41	1.47	3520.153	0.004	3.098	0.001	0.005
4200	14.11	1.82	4506.013	0.005	3.965	0.001	0.007
4800	14.81	2.18	5555.135	0.006	4.889	0.001	0.008
5400	15.52	2.53	6669.114	0.007	5.869	0.001	0.010
6000	15.88	2.71	7250.929	0.007	6.381	0.001	0.011
6600	16.41	2.97	8155.260	0.008	7.177	0.001	0.012
7200	16.95	3.24	9098.140	0.009	8.006	0.001	0.007
8400	17.66	3.60	10416.500	0.010	9.167	0.000	0.008
9600	18.02	3.78	11102.379	0.011	9.770	0.000	0.008
10800	18.02	3.78	11102.379	0.011	9.770		

Appendix F Thickness With 1200 PPM of PEVA

Table F1 Evolution of thickness at $T_{jac} = 45\text{ }^{\circ}\text{C}$, $\Delta T = 40\text{ }^{\circ}\text{C}$, rpm=135, $t = 2\text{ hr}$ with 1200 PPM P-EVA

t(sec)	diameter(mm)	Thickness(mm)	Volume(mm ³)	Volume(L)	mass(g)	Rate (mm/sec)	Mass Rate(g/sec)
0	10.46	0.000	0.000	0.000	0.000	0.000	0.000
2	10.98	0.258	545.395	0.001	0.480	0.207	0.160
5	11.50	0.517	1122.509	0.001	0.988	0.151	0.198
10	12.19	0.863	1942.417	0.002	1.709	0.151	0.171
20	13.76	1.648	4005.274	0.004	3.525	0.105	0.352
30	14.29	1.911	4762.301	0.005	4.191	0.044	0.419
40	14.64	2.087	5286.837	0.005	4.652	0.026	0.465
50	14.81	2.175	5555.135	0.006	4.889	0.018	0.489
60	14.99	2.264	5827.487	0.006	5.128	0.018	0.513
70	15.17	2.352	6103.917	0.006	5.371	0.018	0.537
80	15.34	2.441	6384.451	0.006	5.618	0.009	0.562
90	15.34	2.441	6384.451	0.006	5.618	0.009	0.562
100	15.52	2.529	6669.114	0.007	5.869	0.018	0.587
110	15.70	2.618	6957.932	0.007	6.123	0.009	0.612
120	15.70	2.618	6957.932	0.007	6.123	0.009	0.612
130	15.88	2.706	7250.929	0.007	6.381	0.012	0.319
150	16.05	2.795	7548.133	0.008	6.642	0.009	0.332
170	16.23	2.884	7849.568	0.008	6.908	0.009	0.345
190	16.41	2.973	8155.260	0.008	7.177	0.007	0.239
220	16.59	3.062	8465.235	0.008	7.449	0.004	0.372
240	16.59	3.062	8465.235	0.008	7.449	0.004	0.372
260	16.77	3.152	8779.520	0.009	7.726	0.003	0.193
300	16.77	3.152	8779.520	0.009	7.726	0.000	0.129
360	16.77	3.152	8779.520	0.009	7.726	0.001	0.129
420	16.95	3.241	9098.140	0.009	8.006	0.002	0.067
540	17.12	3.330	9421.122	0.009	8.291	0.001	0.069
660	17.12	3.330	9421.122	0.009	8.291	0.000	0.035
900	17.12	3.330	9421.122	0.009	8.291	0.000	0.028
1200	17.12	3.330	9421.122	0.009	8.291	0.000	0.028
1500	17.12	3.330	9421.122	0.009	8.291	0.000	0.028
1800	17.12	3.330	9421.122	0.009	8.291	0.000	0.014
2400	17.12	3.330	9421.122	0.009	8.291	0.000	0.014
3000	17.30	3.420	9748.491	0.010	8.579	0.000	0.014
3600	17.30	3.420	9748.491	0.010	8.579	0.000	0.014
4200	17.30	3.420	9748.491	0.010	8.579	0.000	0.014
4800	17.30	3.420	9748.491	0.010	8.579	0.000	0.014
5400	17.30	3.420	9748.491	0.010	8.579	0.000	0.014
6000	17.48	3.509	10080.275	0.010	8.871	0.000	0.015
6600	17.48	3.509	10080.275	0.010	8.871	0.000	0.015
7200	17.48	3.509	10080.275	0.010	8.871		

Appendix G Thickness When Wax Content Changes

Table G1 Evolution of thickness 1%wax at $T_{jac} = 45\text{ }^{\circ}\text{C}$, $\Delta T=40\text{ }^{\circ}\text{C}$, rpm=135, t= 2hr

t(sec)	diameter(mm)	Thickness(mm)	Volume(mm ³)	Volume(L)	mass(g)	Rate (mm/sec)	Mass Rate(g/sec)
0	10.46	0.000	0.000	0.000	0.000	0.000	0.000
2	10.81	0.172	360.103	0.000	0.317	0.069	0.106
5	10.81	0.172	360.103	0.000	0.317	0.022	0.063
10	10.98	0.258	545.395	0.001	0.480	0.023	0.048
20	11.15	0.344	734.211	0.001	0.646	0.009	0.065
30	11.15	0.344	734.211	0.001	0.646	0.009	0.065
40	11.32	0.430	926.575	0.001	0.815	0.009	0.082
50	11.32	0.430	926.575	0.001	0.815	0.009	0.082
60	11.50	0.517	1122.509	0.001	0.988	0.017	0.099
70	11.67	0.603	1322.037	0.001	1.163	0.009	0.116
80	11.67	0.603	1322.037	0.001	1.163	0.009	0.116
90	11.84	0.690	1525.182	0.002	1.342	0.009	0.134
100	11.84	0.690	1525.182	0.002	1.342	0.000	0.134
110	11.84	0.690	1525.182	0.002	1.342	0.000	0.134
120	11.84	0.690	1525.182	0.002	1.342	0.009	0.134
130	12.02	0.776	1731.967	0.002	1.524	0.006	0.076
150	12.02	0.776	1731.967	0.002	1.524	0.000	0.076
170	12.02	0.776	1731.967	0.002	1.524	0.000	0.076
190	12.02	0.776	1731.967	0.002	1.524	0.003	0.051
220	12.19	0.863	1942.417	0.002	1.709	0.003	0.085
240	12.19	0.863	1942.417	0.002	1.709	0.000	0.085
260	12.19	0.863	1942.417	0.002	1.709	0.003	0.043
300	12.36	0.950	2156.554	0.002	1.898	0.002	0.032
360	12.36	0.950	2156.554	0.002	1.898	0.000	0.032
420	12.36	0.950	2156.554	0.002	1.898	0.000	0.016
540	12.36	0.950	2156.554	0.002	1.898	0.000	0.016
660	12.36	0.950	2156.554	0.002	1.898	0.000	0.008
900	12.36	0.950	2156.554	0.002	1.898	0.000	0.006
1200	12.36	0.950	2156.554	0.002	1.898	0.000	0.006
1500	12.36	0.950	2156.554	0.002	1.898	0.000	0.006
1800	12.36	0.950	2156.554	0.002	1.898	0.000	0.003
2400	12.54	1.037	2374.402	0.002	2.089	0.000	0.003
3000	12.54	1.037	2374.402	0.002	2.089	0.000	0.003
3600	12.54	1.037	2374.402	0.002	2.089	0.000	0.003
4200	12.54	1.037	2374.402	0.002	2.089	0.000	0.003
4800	12.54	1.037	2374.402	0.002	2.089	0.000	0.003
5400	12.54	1.037	2374.402	0.002	2.089	0.000	0.003
6000	12.54	1.037	2374.402	0.002	2.089	0.000	0.000
226800	12.89	1.211	2821.329	0.003	2.483	0.002	0.000

Table G2 Evolution of thickness 2.5% wax at $T_{jac} = 45\text{ }^{\circ}\text{C}$, $\Delta T = 40\text{ }^{\circ}\text{C}$, rpm=135, t=2hr

t(sec)	diameter(mm)	Thickness(mm)	Volume(mm ³)	Volume(L)	mass(g)	Rate (mm/sec)	Mass Rate(g/sec)
0	10.46	0.000	0.000	0.000	0.000	0.000	0.000
2	11.67	0.603	1322.037	0.001	1.163	0.104	0.065
20	12.54	1.037	2374.402	0.002	2.089	0.037	0.209
30	12.71	1.124	2595.986	0.003	2.284	0.017	0.228
40	12.89	1.211	2821.329	0.003	2.483	0.002	0.004
600	13.93	1.736	4253.679	0.004	3.743	0.001	0.006
1200	14.11	1.823	4506.013	0.005	3.965	0.000	0.007
1800	14.11	1.823	4506.013	0.005	3.965	0.000	0.002
3600	14.11	1.823	4506.013	0.005	3.965	0.000	0.002
5700	14.11	1.823	4506.013	0.005	3.965	0.000	0.013
6000	14.11	1.823	4506.013	0.005	3.965	0.000	0.013
6300	14.11	1.823	4506.013	0.005	3.965	0.000	0.013
6600	14.11	1.823	4506.013	0.005	3.965	0.000	0.007
7200	14.11	1.823	4506.013	0.005	3.965		

Appendix H Thickness When RPM is Switched

Table H1 Evolution of thickness $T_{jac} = 45\text{ }^{\circ}\text{C}$, $\Delta T = 40\text{ }^{\circ}\text{C}$, rpm=240 1hr and rpm=0 1hr

t(sec)	diameter(mm)	Thickness	Volume(mm ³)	Volume(L)	mass(g)	Rate (mm/sec)	Mass Rate(g/sec)
0	10.5	0.000	0.000	0.000	0.000	0.000	0.000
2	11.7	0.603	1322.037	0.001	1.163	0.155	0.155
5	12.0	0.776	1731.967	0.002	1.524	0.043	0.043
10	12.4	0.950	2156.554	0.002	1.898	0.023	0.023
20	12.7	1.124	2595.986	0.003	2.284	0.022	0.022
30	13.2	1.385	3283.388	0.003	2.889	0.017	0.017
40	13.4	1.473	3520.153	0.004	3.098	0.009	0.009
50	13.6	1.560	3760.774	0.004	3.309	0.013	0.013
60	13.9	1.736	4253.679	0.004	3.743	0.013	0.013
70	14.1	1.823	4506.013	0.005	3.965	0.009	0.009
80	14.3	1.911	4890.268	0.005	4.303	0.009	0.009
90	14.5	1.999	5139.262	0.005	4.523	0.009	0.009
100	14.6	2.087	5391.578	0.005	4.745	0.009	0.009
110	14.8	2.175	5647.226	0.006	4.970	0.004	0.004
120	14.8	2.175	5647.226	0.006	4.970	0.000	0.000
130	14.8	2.175	5647.226	0.006	4.970	0.000	0.000
150	14.8	2.175	5647.226	0.006	4.970	0.002	0.002
170	15.0	2.264	5906.215	0.006	5.197	0.002	0.002
190	15.0	2.264	5906.215	0.006	5.197	0.000	0.000
220	15.0	2.264	5906.215	0.006	5.197	0.002	0.002
240	15.2	2.352	6168.556	0.006	5.428	0.002	0.002
260	15.2	2.352	6168.556	0.006	5.428	0.000	0.000
300	15.2	2.352	6168.556	0.006	5.428	0.000	0.000
360	15.2	2.352	6168.556	0.006	5.428	0.001	0.001
420	15.3	2.441	6434.258	0.006	5.662	0.000	0.000
540	15.3	2.441	6434.258	0.006	5.662	0.000	0.000
660	15.3	2.441	6434.258	0.006	5.662	0.000	0.000
900	15.5	2.529	6703.331	0.007	5.899	0.000	0.000
1200	15.5	2.529	6703.331	0.007	5.899	0.000	0.000
1500	15.7	2.618	6975.786	0.007	6.139	0.000	0.000
1800	15.9	2.706	7251.632	0.007	6.381	0.000	0.000
2400	15.9	2.706	7251.632	0.007	6.381	0.000	0.000
3000	15.9	2.706	7251.632	0.007	6.381	0.000	0.000
3600	15.9	2.706	7251.632	0.007	6.381	0.003	0.003
3660	16.9	3.241	8978.486	0.009	7.901	0.004	0.004
3720	18.9	4.229	12469.587	0.012	10.973	0.003	0.003
3840	20.9	5.230	16392.958	0.016	14.426	0.002	0.002
3960	22.4	5.964	19525.585	0.020	17.183	0.001	0.001
4080	23.3	6.426	21605.579	0.022	19.013	0.001	0.001
4200	23.9	6.705	22899.322	0.023	20.151	0.004	0.004
4800	26.3	7.921	28909.629	0.029	25.440	0.001	0.001
5400	26.7	8.110	29893.519	0.030	26.306	0.000	0.000
6000	27.3	8.394	31399.444	0.031	27.632	0.000	0.000
6600	27.4	8.488	31909.485	0.032	28.080	0.000	0.000
7200	27.6	8.583	32423.577	0.032	28.533		

Table H2 Evolution of thickness $T_{jac} = 45\text{ }^{\circ}\text{C}$, $\Delta T=40\text{ }^{\circ}\text{C}$, rpm=0 1.5hr and rpm=240 1.5hr

t(sec)	diameter(mm)	Thickness(mm)	Volume(mm ³)	Volume(L)	mass(g)	Rate (mm/sec)	Mass Rate(g/sec)
0	10.5	0.00	0.000	0.000	0.000	0.000	0.000
2	12.4	0.95	2156.554	0.002	1.898	0.207	0.207
5	12.5	1.04	2374.402	0.002	2.089	0.044	0.044
10	13.1	1.30	3050.455	0.003	2.684	0.041	0.041
20	13.8	1.65	4005.274	0.004	3.525	0.031	0.031
30	14.3	1.91	4762.301	0.005	4.191	0.026	0.026
40	14.8	2.18	5555.135	0.006	4.889	0.031	0.031
50	15.5	2.53	6669.114	0.007	5.869	0.027	0.027
60	15.9	2.71	7250.929	0.007	6.381	0.018	0.018
70	16.2	2.88	7849.568	0.008	6.908	0.027	0.027
80	16.9	3.24	8978.486	0.009	7.901	0.031	0.031
90	17.5	3.51	9888.504	0.010	8.702	0.018	0.018
100	17.7	3.60	10198.814	0.010	8.975	0.009	0.009
110	17.8	3.69	10512.624	0.011	9.251	0.009	0.009
120	18.0	3.78	10829.947	0.011	9.530	0.004	0.004
130	18.0	3.78	10829.947	0.011	9.530	0.015	0.015
150	18.9	4.23	12469.587	0.012	10.973	0.011	0.011
170	18.9	4.23	12469.587	0.012	10.973	0.005	0.005
190	19.3	4.41	13150.378	0.013	11.572	0.009	0.009
220	19.8	4.68	14198.536	0.014	12.495	0.009	0.009
240	20.2	4.86	14915.408	0.015	13.126	0.009	0.009
260	20.6	5.05	15646.855	0.016	13.769	0.008	0.008
300	21.1	5.32	16771.532	0.017	14.759	0.005	0.005
360	21.5	5.50	17539.774	0.018	15.435	0.006	0.006
420	22.6	6.06	19934.008	0.020	17.542	0.006	0.006
540	23.7	6.61	22464.238	0.022	19.769	0.004	0.004
660	24.4	6.98	24227.720	0.024	21.320	0.003	0.003
900	25.6	7.55	26989.610	0.027	23.751	0.002	0.002
1200	26.5	8.02	29399.575	0.029	25.872	0.001	0.001
1500	27.1	8.30	30893.443	0.031	27.186	0.001	0.001
1800	27.6	8.58	32423.577	0.032	28.533	0.001	0.001
2400	28.0	8.77	33463.957	0.033	29.448	0.000	0.000
3000	28.1	8.82	33713.455	0.034	29.668	0.000	0.000
3600	28.2	8.87	33990.605	0.034	29.912	0.000	0.000
4200	28.4	8.96	34520.668	0.035	30.378	0.000	0.000
4800	28.6	9.06	35055.174	0.035	30.849	0.000	0.000
5400	29.0	9.25	36136.543	0.036	31.800	-0.005	-0.005
5700	28.6	9.06	35055.174	0.035	30.849	-0.005	-0.005
5760	27.4	8.49	31909.485	0.032	28.080	-0.004	-0.004
5770	26.3	7.92	28909.629	0.029	25.440	-0.003	-0.003
5790	22.8	6.15	20346.208	0.020	17.905	-0.003	-0.003
5820	22.8	6.15	20346.208	0.020	17.905	-0.001	-0.001
5880	19.8	4.68	14198.536	0.014	12.495	-0.001	-0.001
5940	18.4	3.96	11475.167	0.011	10.098	-0.002	-0.002
6000	17.1	3.33	9278.350	0.009	8.165	-0.005	-0.005
6600	16.2	2.88	7813.539	0.008	6.876	0.000	0.000
7200	16.2	2.88	7813.539	0.008	6.876	0.000	0.000
7800	16.2	2.88	7813.539	0.008	6.876	0.000	0.000
8400	16.2	2.88	7813.539	0.008	6.876	0.000	0.000
9000	16.2	2.88	7813.539	0.008	6.876	0.000	0.000
9600	16.2	2.88	7813.539	0.008	6.876	0.000	0.000
10200	16.2	2.88	7813.539	0.008	6.876	0.000	0.000
10800	16.2	2.88	7813.539	0.008	6.876		

Appendix I Interface Temperature, T_i by Experiment

Table I1 Interface temperature $T_{jac} = 45\text{ }^\circ\text{C}$, $\Delta T = 40\text{ }^\circ\text{C}$, rpm=135

time	T_i	T_b	r_i	r_b
0	42.1	44	7.1	14.3
10	40.1	43.9	7.1	14.3
20	38.8	43.9	7.1	14.3
30	43.3	43.8	7.1	14.3
40	41.3	43.8	7.1	14.3
50	40.2	43.7	7.1	14.3
60	40.1	43.7	7.1	14.3
70	43.1	43.7	7.1	14.3
80	43.3	43.6	7.1	14.3
90	42	43.6	7.1	14.3
100	41.5	43.5	7.1	14.3
110	43	43.5	7.1	14.3
120	42.9	43.5	7.1	14.3
130	42.5	43.5	7.1	14.3
140	42.5	43.5	7.1	14.3
150	42.7	43.5	7.1	14.3
160	42.7	43.5	7.1	14.3
170	42.5	43.4	7.1	14.3
180	42.6	43.4	7.1	14.3
190	42.5	43.4	7.1	14.3
200	42.3	43.4	7.1	14.3
210	42	43.4	7.1	14.3
220	41.8	43.4	7.1	14.3
230	41.4	43.4	7.1	14.3
240	41.4	43.4	7.1	14.3
250	41.1	43.4	7.1	14.3
260	41.1	43.4	7.1	14.3
270	41.1	43.4	7.1	14.3
280	41.5	43.4	7.1	14.3
290	41.4	43.4	7.1	14.3
300	41.6	43.4	7.1	14.3
330	42	43.4	7.1	14.3
360	41.4	43.4	7.1	14.3
390	38	43.4	7.1	14.3
420	37.2	43.4	7.1	14.3
450	41.6	43.4	7.1	14.3

480	39.6	43.4	7.1	14.3
510	40.9	43.4	7.1	14.3
540	42.7	43.4	7.1	14.3
600	41.5	43.4	7.1	14.3
630	42.6	43.4	7.1	14.3
660	41.9	43.4	7.1	14.3
690	41.4	43.4	7.1	14.3
720	42.6	43.4	7.1	14.3
750	42.9	43.4	7.1	14.3
780	42	43.4	7.1	14.3
810	41.2	43.4	7.1	14.3
840	41.7	43.4	7.1	14.3
870	41.5	43.4	7.1	14.3
900	39.1	43.4	7.1	14.3
930	41	43.4	7.1	14.3
960	42.2	43.4	7.1	14.3
1020	41.4	43.4	7.1	14.3
1080	40.4	43.4	7.1	14.3
1140	40.1	43.4	7.1	14.3
1200	40.4	43.4	7.1	14.3
1260	42.5	43.4	7.1	14.3
1320	40.2	43.4	7.1	14.3
1380	38.5	43.5	7.1	14.3
1440	39.5	43.5	7.1	14.3
1500	40.3	43.5	7.1	14.3
1560	42.3	43.4	7.1	14.3
1620	41.7	43.4	7.1	14.3
1680	41.1	43.4	7.1	14.3
Exp2	40			
Average	41.38154	43.47344		
STD.	1.28695	0.141689		

Table I2 Interface temperature $T_{jac} = 45\text{ }^{\circ}\text{C}$, $\Delta T=40\text{ }^{\circ}\text{C}$, rpm=240

	Temperature (C)				Radius(mm)
	Min	Max	Average	STD.	
Tw	43.1	43.2	43.15	0.05	26.38
Tb1	43	43.1	43.05	0.05	22.76
Tb2	43	43.1	43.05	0.05	14.46
Tb3	43	43.1	43.05	0.05	9.78
Ti	37.3	42.8	40.575	1.863067	6.90

Table I3 Interface temperature $T_{jac} = 45\text{ }^{\circ}\text{C}$, $\Delta T=30\text{ }^{\circ}\text{C}$, rpm=135

	Temperature (C)				Radius(mm)
	Min	Max	Average	STD.	
Tw	43.1	43.4	43.25	0.15	25.37
Tb1	43.2	43.3	43.25	0.05	20.74
Tb2	43.5	43.8	43.65	0.15	16.23
Tb3	43.1	43.2	43.15	0.05	8.93
Ti	40.8	43.1	41.88	0.78	7.57

Table I4 Interface temperature $T_{jac} = 45\text{ }^{\circ}\text{C}$, $\Delta T=10\text{ }^{\circ}\text{C}$, rpm=135

	Temperature (C)				Radius(mm)
	Min	Max	Average	STD.	
Tw	43.50	43.60	43.55	0.05	27.25
Tb1	43.60	43.70	43.65	0.05	22.58
Tb2	43.50	43.80	43.65	0.15	16.23
Tb3	47.10	43.70	45.40	1.70	7.57
Ti	39.90	40.30	40.14	0.10	5.90

Table I5 Interface temperature $T_{jac} = 50\text{ }^{\circ}\text{C}$, $\Delta T=45\text{ }^{\circ}\text{C}$, rpm=135

	Temperature (C)				Radius(mm)
	Min	Max	Average	STD.	
Tw	47.10	47.20	47.15	0.05	18.02
Tb1	47.10	47.20	47.15	0.05	15.34
Tb2	47.10	47.20	47.15	0.05	12.71
Tb3	47.10	47.20	47.15	0.05	9.61
Ti	38.80	40.90	40.53	1.70	6.90

Table I6 Experimental condition for finding the interface temperature

Column	Condition		
	RPM	Tcf ($^{\circ}\text{C}$)	Tjac
1	135	5	45
2	240	5	45
3	135	15	45
4	135	25	45
5	135	35	45
6	135	5	50

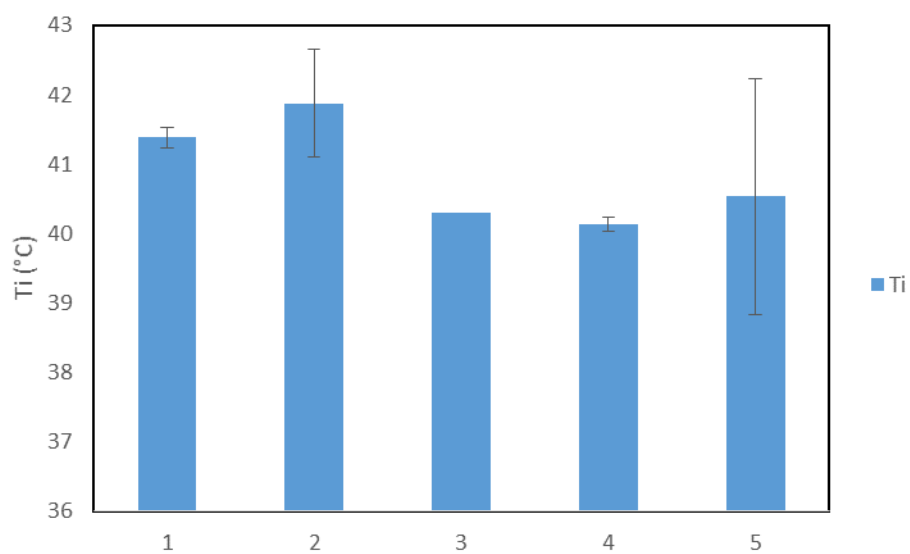
**Figure I1** Interface temperature.

Table I7 Experimental condition for finding the interface temperature when wax content changes

Wax%	Calc Ti (C)	Final Thickness(mm)	Measured WAT(C)
1	29.165	1.04	30
2.5	34.471	1.82	35
5	38.836	3.32	42

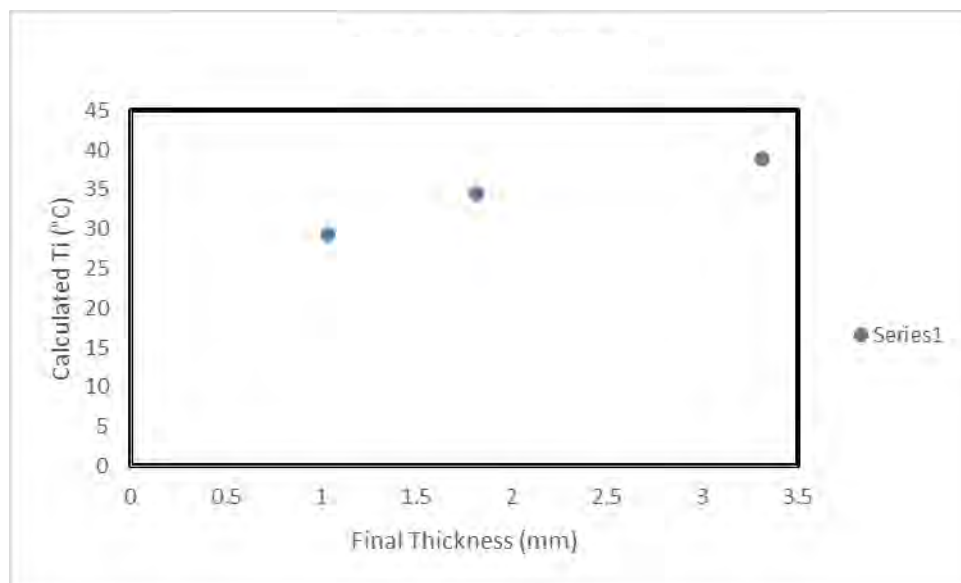


Figure I2 Interface temperature when wax content changes.

Appendix J Temperature Profile by Calculation

Table J1 Temperature profile by calculation

Rc	0.00525	m
rd	0.00845	m
ri	0.00867021	m
re	0.0337833	m
Re	0.034	m
k	0.1	W/mK
L	0.06	m
hjac	460	W/m ² K
hcf	190	W/m ² K

Calculation

R1	12.6246572	K/W
R2	1.65218461	K/W
R3	0.17069034	K/W
Rtotal	14.4475322	K/W
q	2.76863893	W

Rc	0.01	278.00
rd	0.01	312.95
ri	0.01	317.53
re	0.03	317.53
Re	0.03	318.00

T3	317.53	K
T2	312.95	K
T1	278.00	K

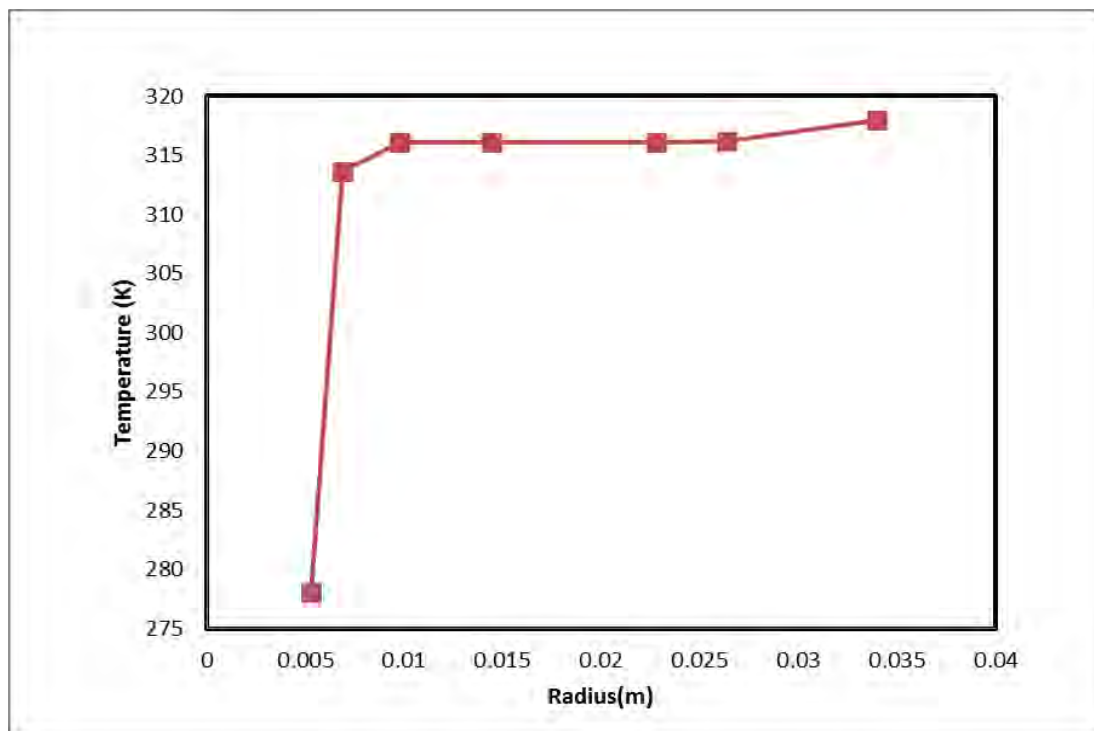


Figure J1 Temperature profile by calculation $T_{jac} = 45\text{ }^{\circ}\text{C}$, $\Delta T = 40\text{ }^{\circ}\text{C}$, rpm=240.

Appendix K Evolution of Thickness Using Primicerio et al. Model

Table K1 Evolution of mass by using Primicerio et al. model

t	$m_w(t)$	$m_w(t)$	$m_{total}(t)$	mass,exp	Mass Diff ²
sec	kg/m ²	g	g	g	g ²
2	-0.002	-0.005	-0.094	0.815	0.826
5	0.004	0.007	0.144	1.492	1.818
10	0.013	0.026	0.527	2.068	2.375
20	0.031	0.062	1.243	2.989	3.048
30	0.048	0.095	1.899	3.312	1.997
40	0.063	0.125	2.499	4.154	2.740
50	0.077	0.152	3.048	4.329	1.640
60	0.090	0.178	3.551	4.506	0.912
70	0.101	0.201	4.011	4.865	0.730
80	0.112	0.222	4.432	5.048	0.380
90	0.122	0.241	4.817	5.233	0.173
100	0.131	0.258	5.169	5.233	0.004
110	0.139	0.275	5.492	5.609	0.014
120	0.146	0.289	5.787	5.609	0.032
130	0.153	0.303	6.057	5.800	0.066
150	0.165	0.327	6.531	6.189	0.116
170	0.175	0.346	6.927	6.189	0.544
190	0.183	0.363	7.259	6.387	0.760
220	0.194	0.383	7.659	6.387	1.617
240	0.199	0.394	7.872	6.587	1.651
260	0.203	0.403	8.051	6.789	1.591
300	0.210	0.416	8.325	6.994	1.774
360	0.217	0.430	8.592	7.409	1.400

420	0.221	0.437	8.748	7.409	1.794
540	0.225	0.445	8.894	7.409	2.206
660	0.226	0.447	8.944	7.620	1.755
900	0.227	0.448	8.968	7.620	1.817
1200	0.227	0.449	8.971	7.833	1.295
1500	0.227	0.449	8.971	8.048	0.851
1800	0.227	0.449	8.971	8.048	0.851
2400	0.227	0.449	8.971	8.048	0.851
3000	0.227	0.449	8.971	8.048	0.851
3600	0.227	0.449	8.971	8.266	0.497
4200	0.227	0.449	8.971	8.266	0.497
4800	0.227	0.449	8.971	8.266	0.497
5400	0.227	0.449	8.971	8.266	0.497
6000	0.227	0.449	8.971	8.266	0.497
6600	0.227	0.449	8.971	8.266	0.497
7200	0.227	0.449	8.971	8.266	0.497

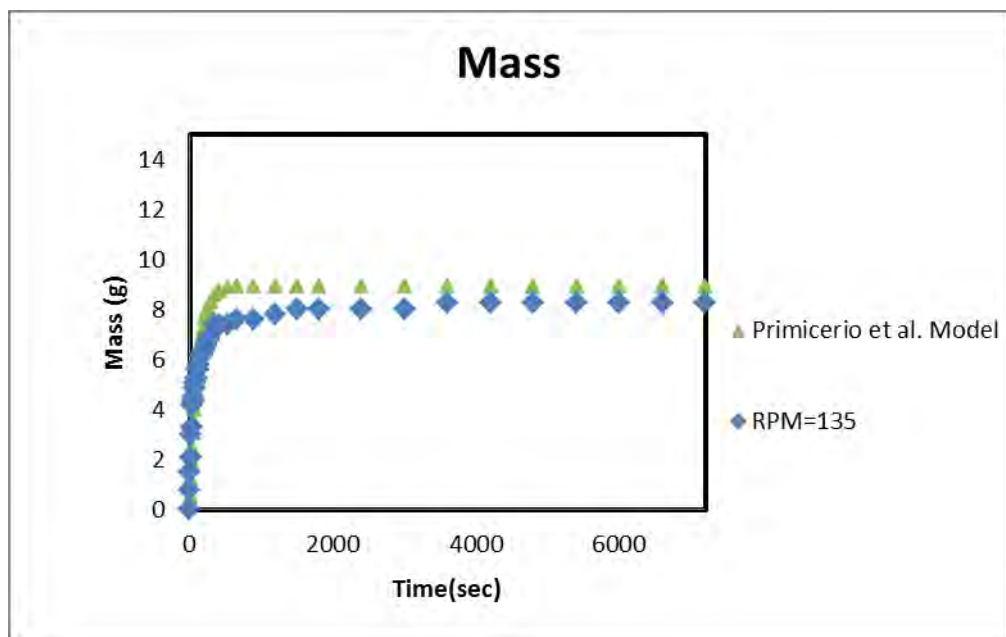


Figure K1 Evolution of mass by Primicerio et al. model.

Appendix L Carbon Number Distribution

Table L1 Carbon number distribution of oil before

1 hr 0.0203 198.46
 3.6878

Before

	Area	RRF	Dillute Con [gn/gw+gm+gT]	Actual Con [gn/gw+gm]
25	31.3	4971956.3	0.000006	0.001145
26	31.9	4704520.4	0.000007	0.001233
27	38.0	4442558.0	0.000009	0.001555
28	42.7	4186069.0	0.000010	0.001854
29	49.1	3935053.3	0.000012	0.002267
30	62.0	3689511.0	0.000017	0.003051
31	88.8	3449442.1	0.000026	0.004677
32	117.3	3214846.6	0.000036	0.006629
33	116.9	2985724.4	0.000039	0.007114
34	97.0	2762075.6	0.000035	0.006383
35	72.6	2543900.3	0.000029	0.005181
36	52.3	2331198.2	0.000022	0.004077
37	35.2	2123969.6	0.000017	0.003008
38	21.9	1922214.4	0.000011	0.002072
39	13.2	1725932.5	0.000008	0.001393
40	8.2	1535124.0	0.000005	0.000965

Table L2 Carbon number distribution of oil after

0.0206 190.281
3.6876

After

	Area	RRF	Dillute Con [gn/gw+gm+gT]	Actual Con [gn/gw+gm]
25	23.75	4971956.25	0.00	0.00
26	24.17	4704520.44	0.00	0.00
27	28.65	4442558.01	0.00	0.00
28	33.16	4186068.96	0.00	0.00
29	36.66	3935053.29	0.00	0.00
30	45.51	3689511.00	0.00	0.00
31	66.20	3449442.09	0.00	0.00
32	87.49	3214846.56	0.00	0.00
33	86.12	2985724.41	0.00	0.01
34	71.49	2762075.64	0.00	0.00
35	53.65	2543900.25	0.00	0.00
36	38.98	2331198.24	0.00	0.00
37	25.79	2123969.61	0.00	0.00
38	15.86	1922214.36	0.00	0.00
39	9.06	1725932.49	0.00	0.00
40	6.38	1535124.00	0.00	0.00

Table L3 Carbon number distribution of wax deposit

0.0218 8.179
3.6892

Deposit				
	Area	RRF	Dillute Con [gn/gw+gm+gT]	Actual Con [gn/gw+gm]
25	27.80	4971956.25	0.00	0.00
26	28.13	4704520.44	0.00	0.00
27	31.54	4442558.01	0.00	0.00
28	36.47	4186068.96	0.00	0.00
29	43.52	3935053.29	0.00	0.00
30	52.55	3689511.00	0.00	0.00
31	85.78	3449442.09	0.00	0.00
32	118.12	3214846.56	0.00	0.01
33	128.78	2985724.41	0.00	0.01
34	119.57	2762075.64	0.00	0.01
35	100.66	2543900.25	0.00	0.01
36	80.88	2331198.24	0.00	0.01
37	58.78	2123969.61	0.00	0.00
38	38.21	1922214.36	0.00	0.00
39	32.93	1725932.49	0.00	0.00
40	15.44	1535124.00	0.00	0.00

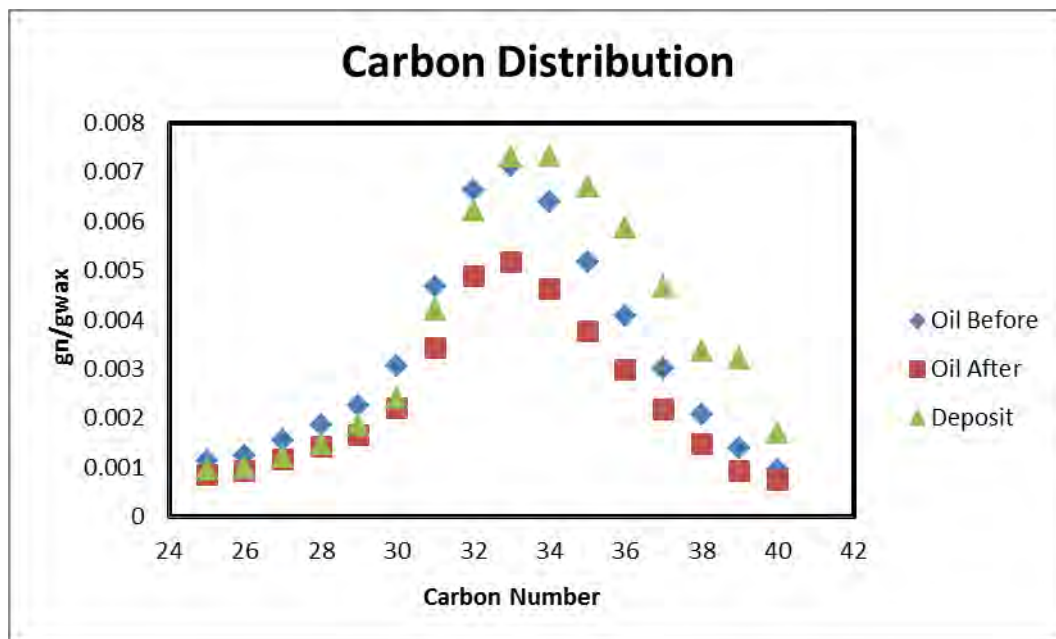
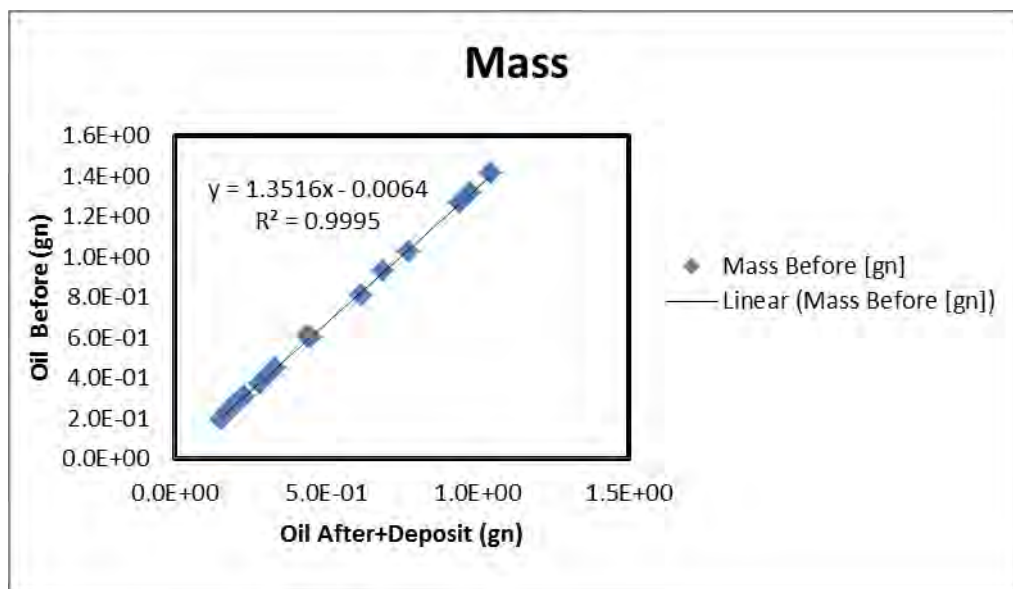


Figure L1 Carbon number distribution of oil before, oil after and deposit.

Table L4 Carbon number distribution of oil before, oil after and deposit

	Mass Before [gn]	Mass After[gn]	%Error
25	2.3E-01	1.7E-01	25.0
26	2.4E-01	1.8E-01	25.1
27	3.1E-01	2.3E-01	25.6
28	3.7E-01	2.8E-01	23.4
29	4.5E-01	3.3E-01	26.1
30	6.1E-01	4.4E-01	27.3
31	9.3E-01	6.9E-01	25.9
32	1.3E+00	9.8E-01	25.7
33	1.4E+00	1.0E+00	26.2
34	1.3E+00	9.4E-01	25.7
35	1.0E+00	7.7E-01	24.8
36	8.1E-01	6.2E-01	23.7
37	6.0E-01	4.5E-01	24.3
38	4.1E-01	3.1E-01	25.0
39	2.8E-01	2.1E-01	25.8
40	1.9E-01	1.6E-01	18.8

**Figure L2** Mass balance of oil before, oil after and deposit.

CURRICULUM VITAE

Name: Ms. Tunya Ketjuntiwa

Date of Birth: August 21, 1991

Nationality: Thai

University Education:

2010-2015 Bachelor Degree of Chemical Engineering, Faculty of Engineering, King Mongkut's Institute of Technology North Bangkok, Bangkok, Thailand

Work Experience:

2013 Position: Engineering Internship (2months)

Company name: Bangchak Petroleum PLC

2013-2014 Position: Exchange student

Company name: The University of Manchester

Proceedings:

1. Ketjuntiwa K., Hakim Ahmad Mahir L. Vilas Bôas Fávero C., Malakul P., and Fogler H. S. (2017, May 23rd) Effects of bead size and concentration of unstable asphaltene obtained from different centrifugation techniques on asphaltene deposition in packed bed apparatus. Proceedings of The 8th Research Symposium on Petrochemical and Material Technology and the 23nd PPC Symposium on Petroleum, Petrochemicals and Polymers, Bangkok, Thailand.